

INFORMATION TO USERS

This dissertation was produced from a microfilm copy of the original document. While the most advanced technological means to photograph and reproduce this document have been used, the quality is heavily dependent upon the quality of the original submitted.

The following explanation of techniques is provided to help you understand markings or patterns which may appear on this reproduction.

1. The sign or "target" for pages apparently lacking from the document photographed is "Missing Page(s)". If it was possible to obtain the missing page(s) or section, they are spliced into the film along with adjacent pages. This may have necessitated cutting thru an image and duplicating adjacent pages to insure you complete continuity.
2. When an image on the film is obliterated with a large round black mark, it is an indication that the photographer suspected that the copy may have moved during exposure and thus cause a blurred image. You will find a good image of the page in the adjacent frame.
3. When a map, drawing or chart, etc., was part of the material being photographed the photographer followed a definite method in "sectioning" the material. It is customary to begin photoing at the upper left hand corner of a large sheet and to continue photoing from left to right in equal sections with a small overlap. If necessary, sectioning is continued again — beginning below the first row and continuing on until complete.
4. The majority of users indicate that the textual content is of greatest value, however, a somewhat higher quality reproduction could be made from "photographs" if essential to the understanding of the dissertation. Silver prints of "photographs" may be ordered at additional charge by writing the Order Department, giving the catalog number, title, author and specific pages you wish reproduced.

University Microfilms

300 North Zeeb Road
Ann Arbor, Michigan 48106

A Xerox Education Company

72-30,381

BINA, Melvin Joseph, 1931-
DIRECT LASER INDUCED EXCITATION OF THE SECOND
VIBRATIONAL LEVEL OF HF.

The University of Arizona, Ph.D., 1972
Aerospace Studies

University Microfilms, A XEROX Company, Ann Arbor, Michigan

DIRECT LASER INDUCED EXCITATION OF THE
SECOND VIBRATIONAL LEVEL OF HF

by

Melvin Joseph Bina

A Dissertation Submitted to the Faculty of the
DEPARTMENT OF AEROSPACE AND MECHANICAL ENGINEERING

In Partial Fulfillment of the Requirements
For the Degree of

DOCTOR OF PHILOSOPHY
WITH A MAJOR IN AEROSPACE ENGINEERING

In the Graduate College
THE UNIVERSITY OF ARIZONA

1 9 7 2

THE UNIVERSITY OF ARIZONA

GRADUATE COLLEGE

I hereby recommend that this dissertation prepared under my direction by Melvin Joseph Bina entitled Direct Laser Induced Excitation of the Second Vibrational Level of HF be accepted as fulfilling the dissertation requirement of the degree of Doctor of Philosophy

Russell E. Petersen
Dissertation Director

May 24, 1972
Date

Russell E. Petersen

After inspection of the final copy of the dissertation, the following members of the Final Examination Committee concur in its approval and recommend its acceptance:*

<u>Russell E. Petersen</u>	<u>May 24, 1972</u>
<u>Marvin D. Martin</u>	<u>May 24, 1972</u>
<u>M. Boxer</u>	<u>May 25th, 1972</u>
<u>John T. Slone, Jr.</u>	<u>25th May 1972</u>
<u>John A. Leavitt</u>	<u>May 25, 1972</u>

*This approval and acceptance is contingent on the candidate's adequate performance and defense of this dissertation at the final oral examination. The inclusion of this sheet bound into the library copy of the dissertation is evidence of satisfactory performance at the final examination.

PLEASE NOTE:

Some pages may have
indistinct print.

Filmed as received.

University Microfilms, A Xerox Education Company

STATEMENT BY AUTHOR

This dissertation has been submitted in partial fulfillment of requirements for an advanced degree at The University of Arizona and is deposited in the University Library to be made available to borrowers under rules of the Library.

Brief quotations from this dissertation are allowable without special permission, provided that accurate acknowledgement of source is made. Requests for permission for extended quotation from or reproduction of this manuscript in whole or in part may be granted by the head of the major department or the Dean of the Graduate College when in his judgment the proposed use of the material is in the interests of scholarship. In all other instances, however, permission must be obtained from the author.

SIGNED:

Melvin J. Bina

DEDICATION

I dedicate this dissertation to my parents, Mr. and Mrs. A. F. Bina, and to my wife, La Donna. My parents supported my interest in science from childhood to my entry into college. My wife has given her untiring support from the days of my undergraduate studies through the writing of this dissertation.

ACKNOWLEDGMENTS

I would like to thank Professor R. E. Petersen for his support throughout the period of this work. In addition to his technical guidance, I am also grateful for his helpfulness on many matters during my absence from the campus. My thanks also to Major J. R. Doughty and Dr. L. E. Wilson for their guidance and support in the conduct of this research. I would particularly like to thank Captain C. R. Jones, who made the original proposal for this research, for his invaluable assistance during all phases of the work. I also want to thank Dr. J. F. Bott for his help in dealing with the HF cell passivation problem. Lieutenant J. J. Lowery provided considerable help with the gas handling system. I am very grateful to the Air Force Institute of Technology and the Air Force Weapons Laboratory for making this endeavor possible. This dissertation was typed by Mrs. Esther Caster.

TABLE OF CONTENTS

	Page
LIST OF ILLUSTRATIONS	vi
LIST OF TABLES	viii
ABSTRACT	ix
1. INTRODUCTION	1
2. BACKGROUND AND PREVIOUS INVESTIGATIONS	7
Mechanisms of Molecular Vibrational Relaxation	7
Previous Investigations	15
3. LASER DEVELOPMENT	24
The Nd:Glass Laser	24
The Nd:YALO and Nd:YAG Laser	32
Wavelength Versus Temperature Dependence of YALO	35
Energy Enhancement Techniques	41
4. EXPERIMENTAL TECHNIQUES	56
5. RESULTS AND CONCLUSIONS	69
Data Interpretation and Results	69
Conclusions	76
APPENDIX A: HYDROGEN FLUORIDE GAS HANDLING SYSTEM	78
APPENDIX B: THE HF PIN LASER	85
APPENDIX C: THE INFRARED DETECTOR SYSTEM	90
APPENDIX D: CALCULATION OF THE ENERGY REQUIREMENTS OF THE EXCITATION LASER	94
LIST OF SYMBOLS	100
REFERENCES	103

LIST OF ILLUSTRATIONS

Figure	Page
2.1 Relative Production Rates for HF Vibrational Levels	9
2.2 A Landau-Teller Plot Showing the Results of Experimental and Theoretical Work on the V=1 Level of HF	18
2.3 A Schematic of the Vibrational-Rotational Energy Levels with Relevant Transitions (not to scale) .	22
2.4 Population of the Rotational Levels of the HF in the V=0 Level	23
3.1 General Laser Configuration	27
3.2 Laser Head Details	29
3.3 Laser Configuration With a Prism in the Cavity . .	33
3.4 Wavelength Versus Temperature for Nd:YALO 038 . .	39
3.5 Slope Efficiency Curve for YALO 038	42
3.6 A Typical Long Pulse Mode of the Nd:YALO Laser . .	43
3.7 Q Switch Circuit	45
3.8 Wavelength Versus Temperature With and Without Q Switching	47
3.9 Wavelength Versus Temperature With the HF Cell in the Cavity	50
3.10 Nd:YALO Laser Beam Absorption by the HF Cell . . .	51
3.11 Breakdown of the Wavelength Versus Temperature Dependence of the Nd:YALO 038 Laser	53
3.12 Wavelength Versus Temperature for Nd:YALO P47 . .	55
4.1 Experimental Arrangement	57

LIST OF ILLUSTRATIONS--(Continued)

Figure	Page
4.2 A Typical Nonpumping Nd:YALO Laser Pulse, Operating in the Single Pulse Mode	64
4.3 A Typical Pumping Nd:YALO Laser Pulse Operating in the Single Pulse Mode	65
4.4 Trace 8-2A A Pumping YALO 038 Pulse, Laser in the Long Pulse Mode	66
5.1 A Semi-log Plot of the Data Points from an Oscilloscope Trace Showing the Double Exponential. $T = 300^{\circ}\text{K}$	71
A.1 The HF Gas Handling System	81
A.2 The HF Cell Assembly	82
B.1 The HF Pin Laser	86
B.2 The HF Pin Laser Circuit	88
C.1 The IR Detector Assembly	91

LIST OF TABLES

Table		Page
3.1	Vacuum Wavelength of the Vibration-Rotation Levels of HF	26
3.2	Summary of the Wavelengths Measured for the Various Lasers Tested	36
5.1	Relaxation Times Obtained From the Excitation of the Second Vibrational Level of HF at 300°K . .	73

ABSTRACT

The primary objective of this experiment was to measure the relaxation time of the second vibrational level of gaseous hydrogen fluoride (HF) by means of direct laser induced excitation. The results presented here represent the first reported instance of direct overtone excitation of molecular vibration-rotation energy levels. The successful result was based on the development of a solid state laser, neodymium doped yttrium orthoaluminate, that could be temperature tuned to the proper wavelength to be resonant with the $(V=0 \rightarrow 2)P(6)$ level of HF. The laser beam was directed into an HF cell that operated in conjunction with a gas flow system that supplied pure mixtures of HF in argon at approximate partial pressures of HF of 1 torr. Following laser excitation, the infrared fluorescence from the vibrationally excited HF molecules in the cell was monitored by means of an InSb detector operated at liquid nitrogen temperatures. The temporal decay of the fluorescence was a double exponential and the data recorded by means of an oscilloscope display photograph was transferred to semi-logarithmic plots in order to determine the slope. The two slopes obtained from each plot represented the relaxation of the HF from its second and first vibrationally excited levels. The

accidental destruction of the laser prevented complete investigation, but the data obtained is consistent with that of other investigators. The room temperature average value for HF(V=2→1) was $P\tau_2 = 6.62\mu\text{sec-torr}$ and for HF(V=1→0) was $P\tau_1 = 13.9\mu\text{sec-torr}$. Quantum theory predicts that the vibrational relaxation of a harmonic oscillator should be such that $(\tau_1/\tau_2)_{\text{th}} = 2$. The value obtained in this work, $(\tau_1/\tau_2)_{\text{obs}} = 2.20 \pm .42$ supports this within the reported uncertainty.

CHAPTER 1

INTRODUCTION

One of the most rapidly expanding technologies today is that of the laser (see Chapter 3 for a discussion of laser operation). A relatively new technology, developing from that of the maser of the 1950's, the laser is now used routinely in industry and has perhaps crossed more scientific disciplines than any other technical phenomenon. Research and development on the laser is expanding at what appears to be an ever-increasing rate. These increased efforts are required in order to reach a better understanding of the mechanisms involved and to expand the applications of the laser. One of the many such development programs currently being pursued is that of the high power chemical laser.

The chemical laser has an advantage over other laser devices, for example the gas dynamic laser, because of its high specific power. In a discussion of chemical lasers, Chester (1971) quotes the mass flow efficiency of the hydrogen fluoride (HF) chemical laser as 136 Kjoule/pound versus the value of 2 Kjoule/pound for the gas dynamic lasers. These high operating efficiencies have resulted in considerable interest in chemical laser development.

This increased effort in chemical lasers has generated a need for information on the kinetic energy exchange processes that govern the lifetime of molecular vibrational-rotational excited states. Since the fundamental physical process of the chemical laser is the preferential excitation of upper vibrational levels of the ground electronic level of the lasing molecules, optimization requires a system configuration which enhances the population of these states as much as possible. Therefore, the analysis and design of new laser systems requires the precise knowledge of the relevant reaction mechanisms, and most particularly, the reaction rate constants for these reactions.

In the chemical laser, the excitation or pumping of the upper vibrational levels is accomplished directly through the chemical reaction. One such reaction is



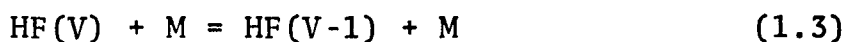
where $n \leq 3$, referred to as the cold reaction, and



where $n \leq 9$, referred to as the hot reaction. These excited molecules can then be used in systems that will either lase

directly or to transfer this excitation to another lasing species.

There are several kinetic processes that will depopulate the upper levels, the most detrimental one being the vibration-translation exchange, (V-T),



where M is any available collision partner including HF. The relaxation rates for the V=1 level are now reasonably well established. However, at this time there are very little data available for the V-T rate with $V > 1$. The rates for $V > 1$ must be determined because of their importance in high power chemical laser development. Of particular importance is the HF(V=2) level since it is the one predominantly populated by the overall reaction.



Also, it is believed that considerable energy redistribution occurs through V-V exchange processes resulting in the populating of the V=2 level from other levels.

Beyond the above mentioned need for information on the HF relaxation rates as they apply to the chemical laser,

is the ever present need for experimental data to help substantiate theoretical studies. Molecular relaxation rates are important in many other non-equilibrium systems besides lasers, for example, blast phenomena, expansion flows, and shock waves. Although a significant amount of progress has been made over the past several years, a review of the literature shows that there are still discrepancies between the experimental findings and the theoretical predictions for many of the molecular reactions of interest.

Measurements of the relaxation rates for the HF have involved work on the first vibrationally excited levels as induced by shock tubes and by direct laser induced excitation using an HF laser. This work has resulted in measurements of the reaction as a function of temperature from 300°K to 4000°K for the first vibrational level. To gain a better insight into the true nature of the collisional deactivation processes that take place, much more research is still needed. Specifically, by selectively activating the higher vibrational levels, a more detailed understanding of the relaxation processes should be possible. The direct result, of course, is the direct rate measurements for the overall relaxation of the upper level.

This experiment was undertaken in an attempt to gain some of the information on the upper vibrational level of HF. Following a discussion in Chapter 2 of the mechanisms involved and the relatively recent background work, Chapter 3 presents what was the main experimental development in this work, that of the excitation laser. As will be seen, this development required greater effort than originally planned and success was achieved as a result of a unique phenomenon that took place in a particular laser material. The unfortunate accidental destruction of this laser terminated the experiment at a time when the usefulness of this method was just starting to be realized. Prior to the loss of the laser, however, direct laser excitation of the second vibrational level of HF was achieved.

The experiment reported here employs for the first time a technique for direct excitation of an overtone ($\Delta V > 1$) transition in HF. Moreover, it is the first reported instance of a vibrational-rotational transition being excited by a laser operating on a different transition or by a laser based upon an entirely different medium than the sample being investigated. Indeed, the method reported herein is a significant and unique extension of the powerful laser-induced fluorescence technique.

The experimental techniques are discussed in Chapter 4 and, in addition to the overall procedures, points out the difficulties that had to be overcome in dealing with the highly reactive HF gas. The room temperature data resulting from the excitation of the second vibrational level that did occur are analyzed and the results and conclusions presented in Chapter 5. Included in this last chapter are recommendations for future work now that the technique of upper level excitation has been proven feasible.

CHAPTER 2

BACKGROUND AND PREVIOUS INVESTIGATIONS

There were two reasons listed in the introduction for the current interest in obtaining data on the relaxation rates for hydrogen fluoride. First, current research in high power chemical lasers requires a knowledge of the rates involved in order to predict laser performance and, second, the data obtained can be used to test theories for vibrational energy transfer. In this chapter, the first section contains a discussion of some of the basic mechanisms involved in molecular energy transfer. The second section discusses previous work on the measurements of HF vibrational relaxation rates.

Mechanisms of Molecular Vibrational Relaxation

The discussion found in this section will address kinetic processes characterizing the HF chemical laser. However, much of the treatment of molecular energy exchange processes applies to other diatomic molecules, since little gas-kinetic research has dealt with HF. For example, there is considerable interest in the hydrogen halides in general and much of the experimental work has been done on HCl since it is not as reactive as HF. The work of Polanyi et al. (1970) and that of Jonathan, Mellior-Smith and Slater (1970)

has demonstrated that as a direct result of chemical reactions, vibrational population inversions can be produced which can maintain lasing action. The reaction between H_2 and F_2 is a good example. Figure 2.1 shows the relative population of the various vibrational levels populated by the two primary HF producing reactions. Note that the hot reaction,



is much less effective in populating vibrational levels and has been found to not produce a significant population inversion, while the cold reaction,



is known to produce inversions that can result in $(V=2 \rightarrow 1)$ and $(V=1 \rightarrow 0)$ lasing. The highly populated $V=2$ level shown in Figure 2.1 graphically points out the need for specific information on the rates associated with the relaxation of this level.

There are several processes that lead to the deactivation of the upper vibrational levels. During laser operation there is the desired result of the deactivation of upper vibrational levels due to stimulated emission. In this process the transition between the upper and lower vibrational

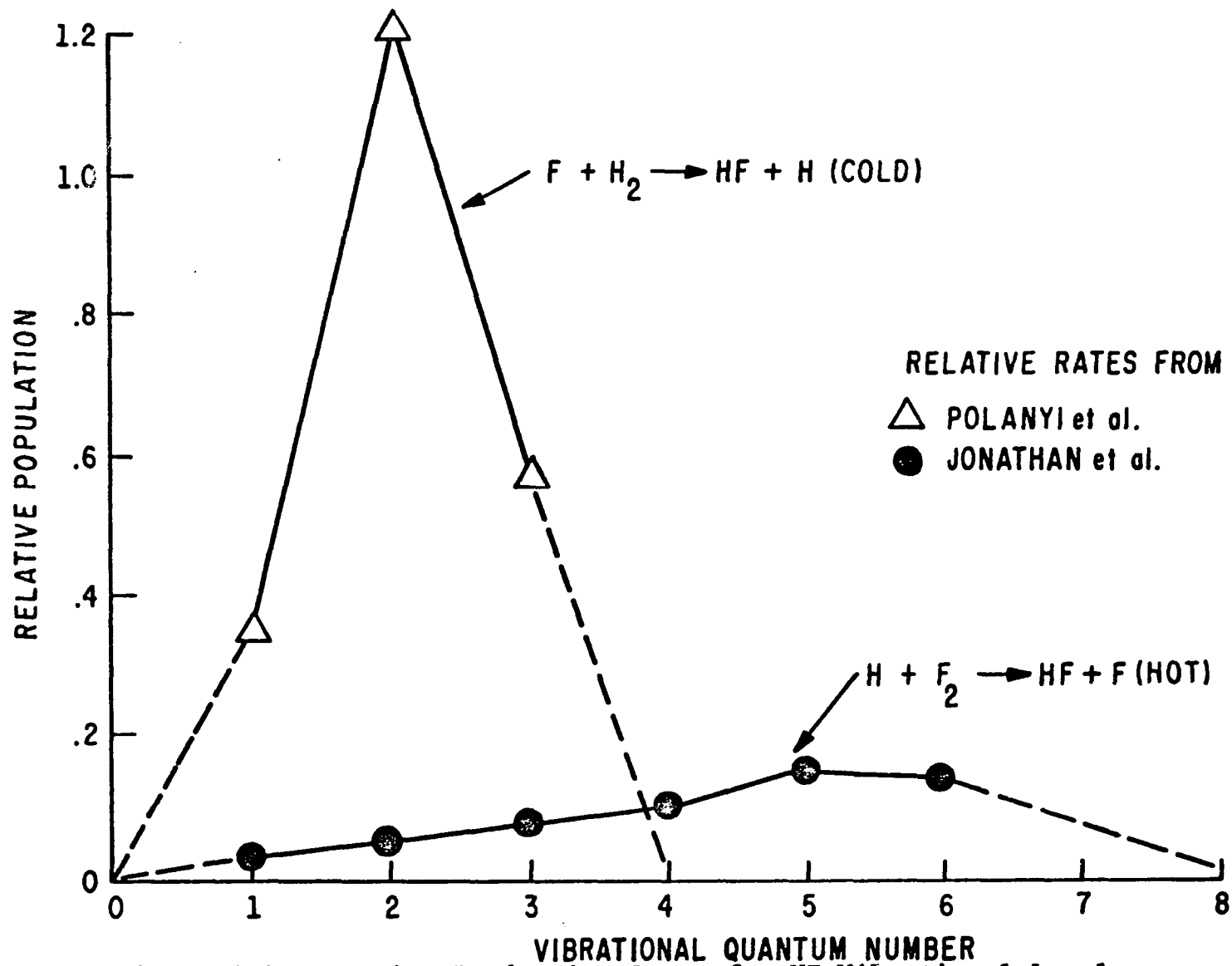
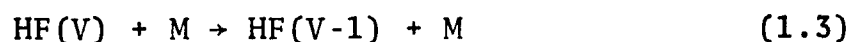


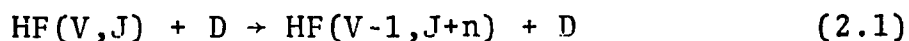
Figure 2.1 Relative Production Rates for HF Vibrational Levels

level is induced by interaction with a photon that meets the resonance requirement of the transition. This induced, or stimulated, transition results in the generation of a second photon identical to the stimulating photon. There is also spontaneous emission occurring from all of the vibrational levels. In the case of HF, spontaneous emission, which is characterized by radiative lifetimes of a few milliseconds, is much slower than the other deactivation processes and is therefore not a significant consideration. Finally, there are the molecular collisional processes that result in a reduction of the desired population inversion. These processes represent a rapid loss of internal molecular energy to the heat bath of the HF laser, competing with the stimulated emission for the stored energy. The molecular collisional losses that occur are the result of three processes, vibration-to-translation energy transfer (V-T), vibration-to-rotation energy transfer (V-R), and vibration-to-vibration energy transfer (V-V). Further, combinations of these three mechanisms can occur, for example, the (V-R-T) process which will be discussed later.

The vibration-to-translation energy transfer can be expressed in the same form as that used in Chapter 1.



where M can be any molecule, including HF. Measurements made by Chen and Moore (1971) of relaxation rates for HCl produced results that were not compatible with vibration-to-translation energy transfer. They suggested that for molecules with large vibrational constants, such as HCl and HF, collisional deactivation that results in large quantities of vibrational energy being converted to translational energy is unlikely. Instead, during a collision, the vibrational energy of the molecule which was originally vibrationally excited is converted into rotational energy. This can be expressed as,



where in this case D is any diatomic molecule. There is little supporting research, but apparently polyatomic and perhaps even atomic collisions would be equally effective. Although there are little experimental data, rotational equilibrium is assumed to occur very rapidly, as is equilibrium between the rotational and translational degrees of freedom. This rotational energy is finally transferred to the translational energy of the molecules. Hence, for a molecule with a large vibrational constant, the most likely energy transfer is probably a vibration-to-rotation-to-translation (V-R-T) sequence.

The remaining collisional energy exchange process is that of vibration-to-vibration energy transfer. This can be expressed as



where D is any diatomic molecule including HF. This is usually a much more rapid process than the (V-R-T) sequence and, in general, it does not lead to a net decrease in vibrational energy, but rather a redistribution of energy among the vibrational levels.

In order to measure the rates at which these various energy exchange processes occur, it is necessary to monitor the rate at which the population of a specific level changes. This can be accomplished by observing the spontaneous emission (fluorescence) of a particular level. For example, to monitor the population of the V=1 level, the fluorescence of the (V=1→0) transition is observed.

The fluorescence from HF(V=2→1) and HF(V=1→0) transitions is nominally 2.7 μm , while the HF(V=2→0) transition, which is a very small fraction of the total, is nominally 1.35 μm . Hence, to monitor this fluorescence requires the use of infrared detection techniques. As mentioned earlier, the energy exchange process deactivating the upper vibrational levels of HF are much more rapid than the spontaneous

emission. Hence, the resulting change in the fluorescence signal as a function of time is a direct measure of these processes. If there are N molecules in the $V=1$ level, then the number of molecules undergoing spontaneous emission is proportional to the number of molecules that remain at any instant,

$$dN/dt = -\gamma N, \quad (2.3)$$

where γ is the rate constant for a collisional reaction. Using the fact that the fluorescence intensity, I , is proportional to the number of molecules undergoing emission, the result is simply

$$I = I_0 e^{-\gamma t}. \quad (2.4)$$

The usual method for expressing the deactivation rate of the vibrational levels is the use of the relaxation time. The relaxation time (or lifetime) is defined as the time it takes for the fluorescence signal to decrease by a factor of $1/e$, and will be written here as τ . From Eq. 2.4 note that

$$\tau = 1/\gamma \quad (2.5)$$

For bimolecular processes, the rate at which the molecular energy transfer takes place is proportional to the pressure of the gas, provided that the concentration of excited molecules is small. This energy transfer is such that the relaxation is exponential with time and the product of the pressure and the relaxation time, expressed as $P\tau$, is constant for a given temperature. The relaxation time is a function of temperature, which depends upon the type of molecular collision involved. A complete theoretical derivation of the functional relationship is complex and will not be repeated here. The most frequently cited result is the expression derived by Landau and Teller (1936). For processes in which the attractive portion of the intermolecular potential dominates, e.g., at low temperatures, they obtained the approximate result

$$P\tau = C \exp(K/T)^{1/3} \quad (2.6)$$

where C and K are constants that depend on the physical properties of the molecule. Note that by plotting $\ln P\tau$ versus $T^{-1/3}$, referred to as a Landau-Teller plot, a straight line will result. In the next section of this chapter a Landau-Teller plot will be used to plot the results of experimental investigations that have been made to determine the relaxation rates of HF as a function of temperature.

Previous Investigations

There are several methods available for exciting the vibrational levels of HF. The most common methods are the use of the shock tube and the technique of direct laser-induced excitation. Each of these methods will be discussed along with a summary of the results currently available as a result of investigations utilizing these methods.

In the shock tube technique vibrationally excited molecules are created in the heated gas just behind the shock wave. The decay of these excited molecules is then observed as a function of time after the passage of the shock wave. In the shock tube there is a minimum temperature needed to ensure that there is a sufficient population of vibrationally excited levels to be able to detect the infrared fluorescence of the gas. Higher pressures can be used to increase the intensity of the fluorescence, but only to the point at which the relaxation time of the HF has decreased to a value that is still four to five times greater than the total response time of the detector system. Thus, because of the short relaxation time of HF and the large energy associated with the first vibrational level, shock tube measurements are limited to temperatures greater than 1300°K.

The first investigators to make use of the shock tube to measure the relaxation rates of HF as a function of temperature were Bott and Cohen (1971). They used a 6-1/2 inch

shock tube with a 35 foot long driven section to measure the value of P_{τ} for HF(V=1) in the temperature range from 1300°K to 4000°K. At about the same time, Solomon et al.(1971), also using a shock tube, measured the values of P_{τ} for HF(V=1) from 1400°K to 4100°K. The results of Bott and Cohen and Solomon et al. are plotted on a Landau-Teller plot along with other results in Figure 2.2 later in this section.

The second commonly used technique for exciting the vibrational levels of HF is the direct laser-induced fluorescence method. This method depends upon the existence of a resonance between an emission line of the exciting laser and the sample to be investigated. To excite the first vibrational level of HF, an HF chemical laser is used to optically excite the same levels in the sample as the levels that the lasing originated from. The laser is operated in a pulsed mode so that all of the excitation takes place in several microseconds. The deactivation of this excited vibrational level is followed by observing the infrared fluorescence.

The first vibrational energy transfer studies using the laser-induced fluorescence technique were done by Hocker et al. (1966) on CO_2 by using a $\text{CO}_2\text{-N}_2\text{-He}$ laser. Moore et al. (1967) continued this research using a similar laser. Airey and Fried (1971) made the first relaxation measurement on HF. The laser in their experiment utilized a lasing medium that was produced by flash photolyzing a mixture of HCl and

OF_2 . They obtained a 350°K value for P_τ of $10.6\mu\text{sec-torr}$ for $\text{HF}(V=1\rightarrow 0)$. This left a temperature gap in the plot of P_τ versus temperature for HF that extended from room temperature to 1300°K .

Bott (1972) has recently combined the laser-induced fluorescence technique with the shock tube. In this method the shock tube is used only as a source of test gas at varying temperatures which can be lower than those practicable in classical shock tube investigations. A test section is positioned at the end of the shock tube such that the laser beam enters the heated gas behind the reflected shock wave. In this manner relaxation rates have been measured for HF ($V=1\rightarrow 0$) as a function of temperature from 300°K to 1000°K .

One of the theories for vibration-rotation-translation energy transfer for HF is that of Shin (1971). Figure 2.2 is a Landau-Teller plot showing his results. Included on Figure 2.2 are the results of Bott (1972), Bott and Cohen (1971), Solomon et al. (1971), and Airey and Fried (1971). As can be seen from the figure, there are still some discrepancies with the theory if an attempt is made to extrapolate the slopes of the experimental data. In general, however, the vibrational relaxation of HF from its first vibrational level has been reasonably well established from 300°K to 4100°K .

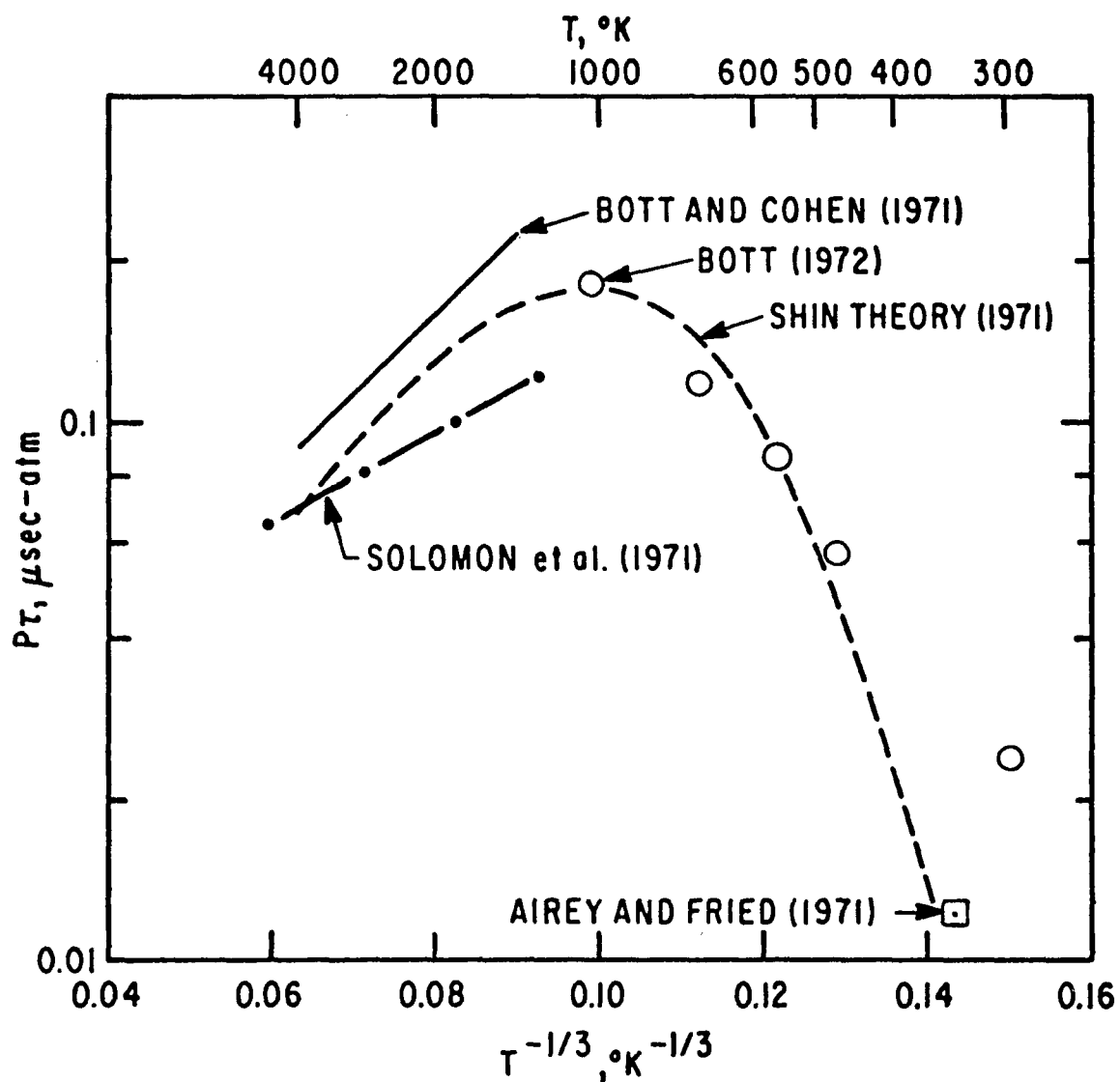
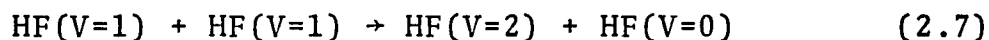


Figure 2.2 A Landau-Teller Plot Showing the Results of Experimental and Theoretical Work on the V=1 Level of HF.

As mentioned earlier, the deactivation rates for HF(V>1) are of critical importance to the chemical laser technology. The recent work of Bott (1972) also included a rate measurement for the V=2 level of HF. This was accomplished by using the HF laser to excite the first vibrational level of the HF in the test cell to a degree such that the (V-V) process transferred sufficient energy into the V=2 level so that its relaxation could be followed. This (V-V) process can be written as



The fluorescence of the V=2 level was observed by passing the total fluorescence through a filter that selectively removed the V(1→0) radiation by absorption on the HF(1→0) lines. The filter consisted of a cell containing HF gas at approximately 100 torr which passed the HF(2→1) fluorescence since there are insufficient molecules at V=1 to absorb this line. The value obtained for the room temperature relaxation time of the second vibrational level of HF was $P\tau(V=2) = 8.9\mu\text{sec-torr}$. Quantum theory predicts for a harmonic oscillator that at constant temperature,

$$VP\tau = \text{Constant} \quad (2.8)$$

This recent result of Bott supports this prediction since the value of $P_{\tau}(V=2)$ is just half of the $P_{\tau}(V=1)$. Nevertheless, it is felt that this technique does not yield entirely unambiguous results. The principal objection is the unavoidable occurrence of collisional transfer of energy into the HF(V=2) level from other vibrational levels, thereby possibly distorting the true HF(V=2) deactivation curve. Hence, a direct excitation of the HF(V=2) level should yield a more exact experiment. Direct excitation of the upper vibrational levels and the resulting measurements of the relaxation rates should provide a test of the validity of Equation (2.8). Moreover, the HF molecule exhibits a considerable degree of anharmonicity and the rates for the higher vibrational levels could differ considerably from the expected results.

The Nd:YALO laser developed for the experiments performed in the present work operated on a wavelength which was resonant with the (V=0 \rightarrow 2) P(6) transition in HF which is characterized by a vacuum wavelength of 1.3404 μ m. Using standard spectroscopic notation, a transition from the ground vibrational level to the second vibrational level will be written as (V=0 \rightarrow 2). The rotational energy level associated with a particular vibrational level is represented by the quantum number J, where J=0,1,2,... Vibrational-rotational transitions where $\Delta J=+1$ in emission are referred to as P(J) transitions and those where $\Delta J=-1$ in emission are referred to

as R(J) transitions. The J value associated with a transition is that of the lower level in emission. Figure 2.3 schematically illustrates the overtone-band transition used in this experiment as well as a typical fundamental-band transition. The spectral lines of these transitions at low pressures, i.e., below a few torr of HF, are predominantly Doppler-broadened since the molecular velocity is more of a factor than its collision rate. At 300°K the line width of a $\Delta V=1$ transition in HF is approximately $\Delta v_D = 300$ megahertz, while for a $\Delta V=2$ transition $\Delta v_D = 600$ megahertz.

For an HF mixture at room temperature the lower level of the pumping transition $V=0, J=6$, contains only a small fraction of the HF molecules. However, at higher temperatures this situation improves and a larger fraction of the molecules are available for excitation. Figure 2.4 shows a plot of the population of the rotational levels for $V=0$ at 300°K and 800°K, this range being typical of operating temperatures for HF lasers. Note that at 300°K only about 2% of the HF molecules are in the P(6) level while this increases to about 10% at 800°K. Higher gas temperatures should improve the capability of the system to measure relaxation rates once it is eventually operated in conjunction with a shock tube.

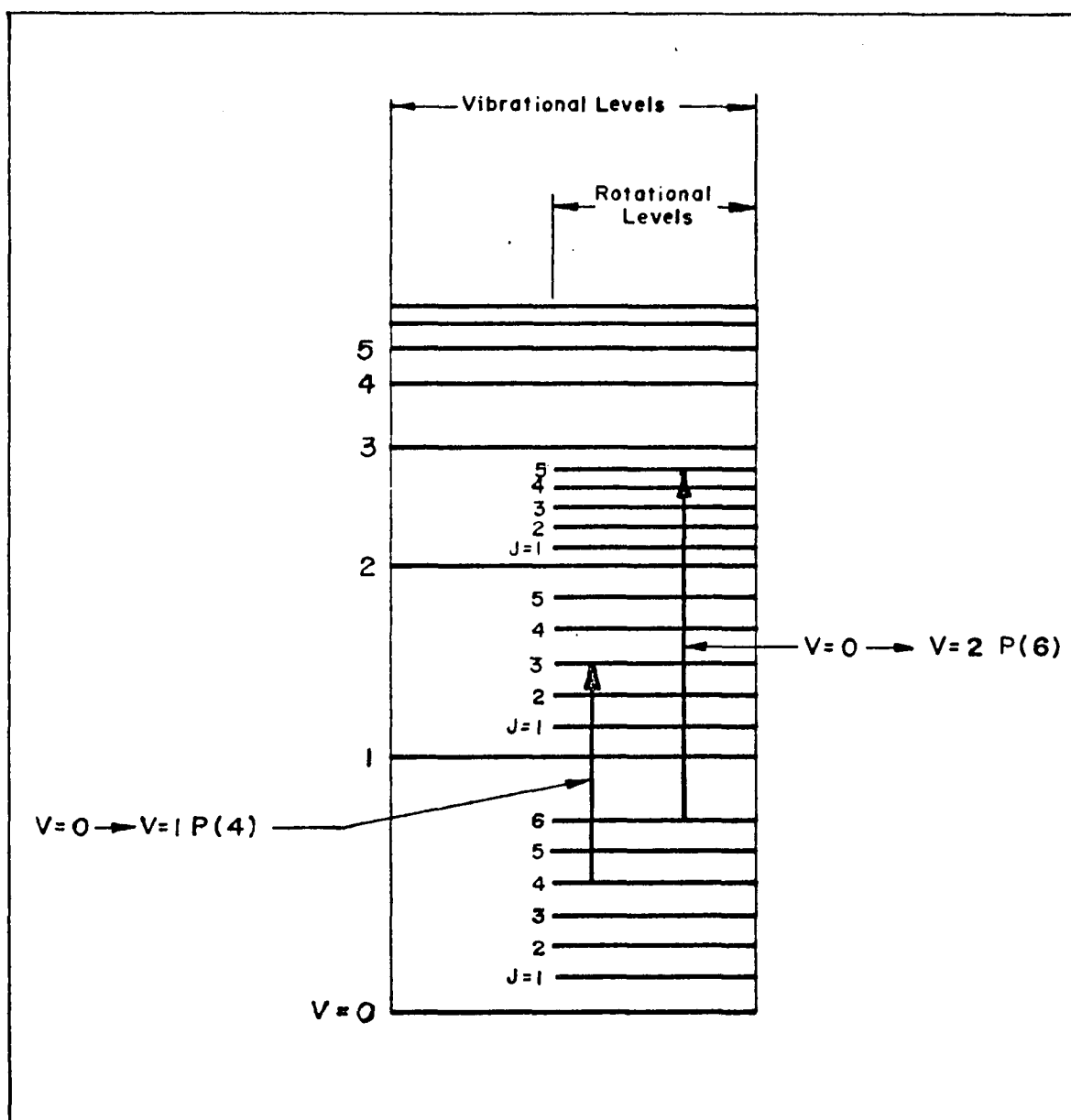


Figure 2.3 A Schematic of the Vibrational-Rotational Energy Levels with Relevant Transitions (not to scale)

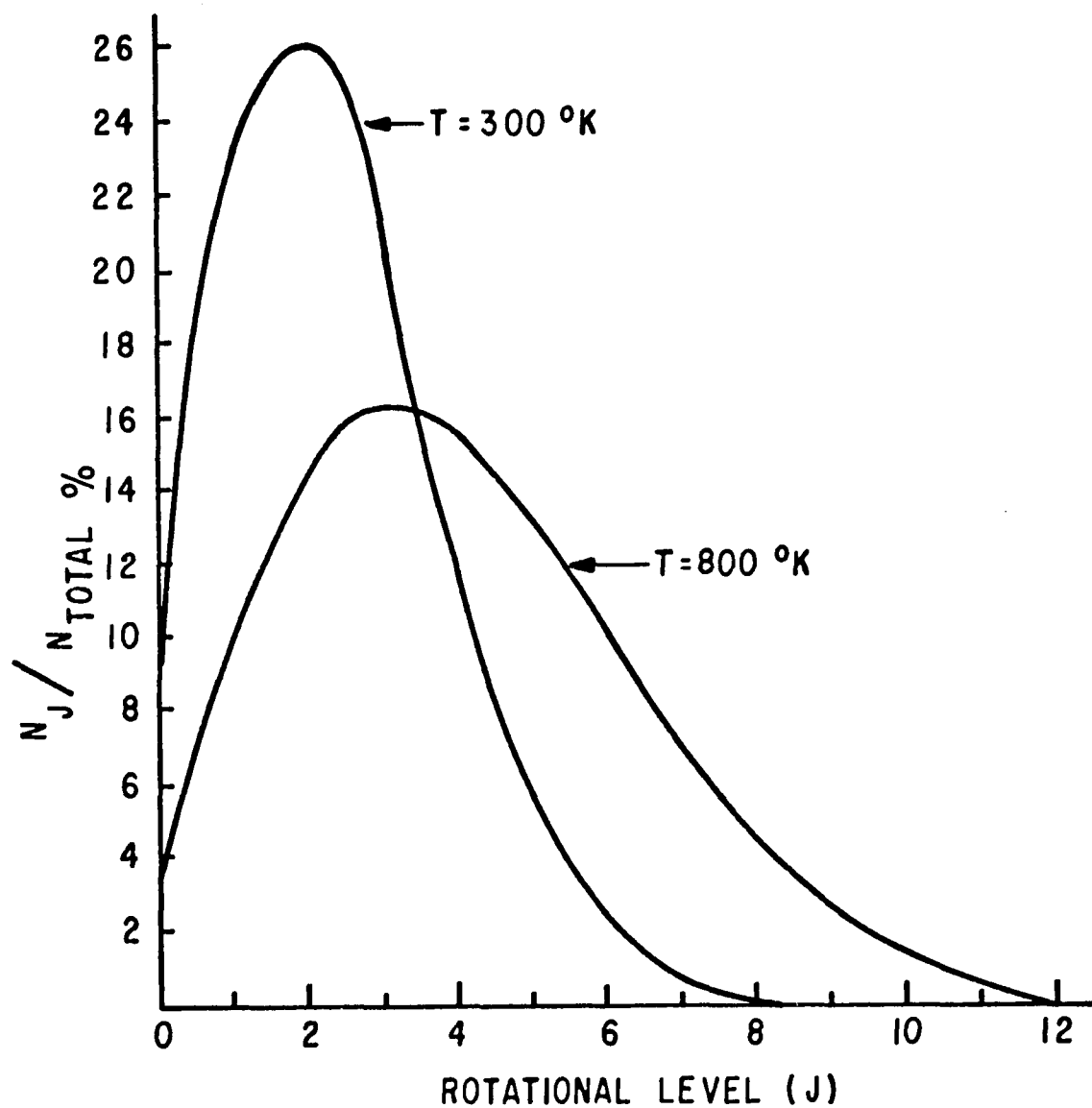


Figure 2.4 Population of the Rotational Levels of HF in the $V=0$ Level

CHAPTER 3

LASER DEVELOPMENT

The previous sections have pointed out the desirability of direct laser excitation of the upper vibrational levels of HF. At first it was thought that the tunable organic dye lasers would be highly suited to this purpose. In an organic dye laser, the lasing medium is an organic fluorescent material dissolved in a common solvent. The nature of these materials is such that they deliver a broad spectral output. However, the longest wavelengths currently available are on the order of $0.9\mu\text{m}$ [see for example Farmer et al. (1969)]. As can be seen from Table 3.1, the dye laser would only be useful for pumping the levels greater than $V=3$. To pump the second vibrational level of HF requires a laser operating on a wavelength in the range of $1.3\mu\text{m}$ to $1.5\mu\text{m}$.

The Nd:Glass Laser

As originally conceived, this experiment was to be carried out using neodymium doped glass (Nd:glass) as the lasing material. The majority of the research carried out on Nd:glass has concentrated on its principle transition lasing at $1.06\mu\text{m}$. However, Pearson, Porto and Northner (1964) report lasing at $1.34\mu\text{m}$ and Snitzer (1966) reports lasing

at $1.37\mu\text{m}$. The amorphous character of glass as a lasing host for the neodymium results in a fairly broad spectral output. This was considered to be an advantage as it was expected that several of the HF ($V=0\rightarrow 2$) rotational levels could be pumped simultaneously.

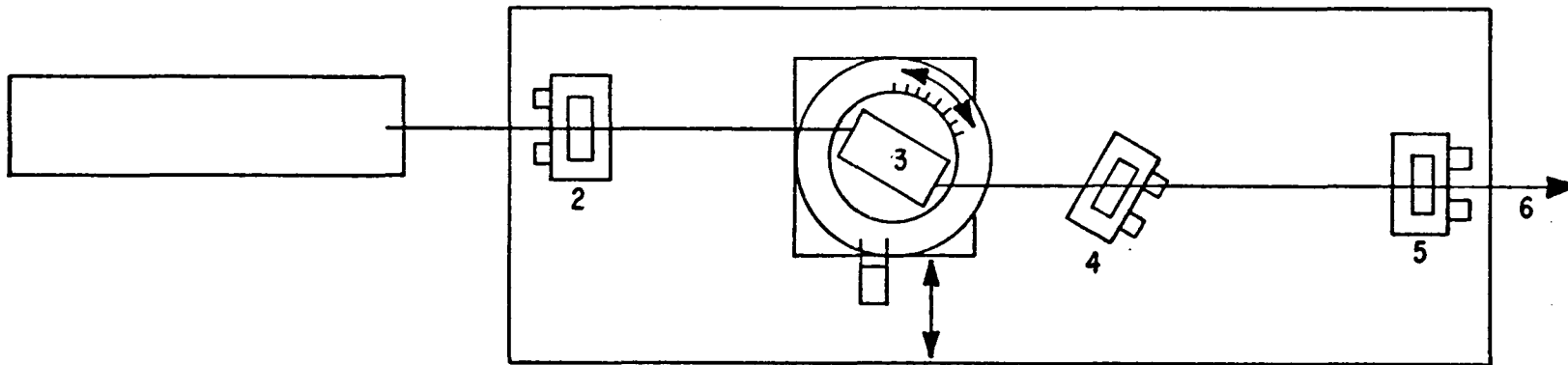
Table 3.1 contains a partial listing of the HF vibration-rotational levels taken from the work of Mann et al. (1961). The rotational line spacing in the region of $1.3\mu\text{m}$ can be seen to be on the order of 100\AA . Thus, a broad band laser operating near $1.34\mu\text{m}$ was expected to pump the second level of HF and Nd:glass seem to offer promise.

A laser system was set up as shown in Figure 3.1. The head was mounted on a base that had a three point suspension for leveling, a micrometer translation adjustment, and a rotational degree of freedom with respect to the laser beam. Details of the laser head are shown in Figure 3.2. Note that in this configuration the beam enters and leaves the lasing material at the Brewster angle to reduce reflection losses. The Brewster angle is that angle of incidence of a light beam with respect to a dielectric where one polarization experiences zero reflection. The helium-neon laser was used to align the laser rod in the head, the orientation of the head, and the mirrors. The space between the mirrors, referred to as the lasing cavity, was approximately 45 inches long. During the firing of the flashlamps,

TABLE 3.1

VACUUM WAVELENGTH OF THE VIBRATION-ROTATION
LEVELS OF HF

(V=0→1) Band - μm	
R(0) - 2.4993	P(1) - 2.5508
(V=0→2) Band - μm	
R(0) - 1.2839	P(1) - 1.2971
	P(2) - 1.3045
	P(3) - 1.3126
	P(4) - 1.3212
	P(5) - 1.3305
	P(6) - 1.3404
	P(7) - 1.3510
(V=0→3) Band - μm	
R(0) - 0.8765	P(1) - 0.8825



- 1. HELIUM-NEON ALIGNMENT LASER
- 2. 99 % 1.35 μ m MIRROR
- 3. LASER HEAD

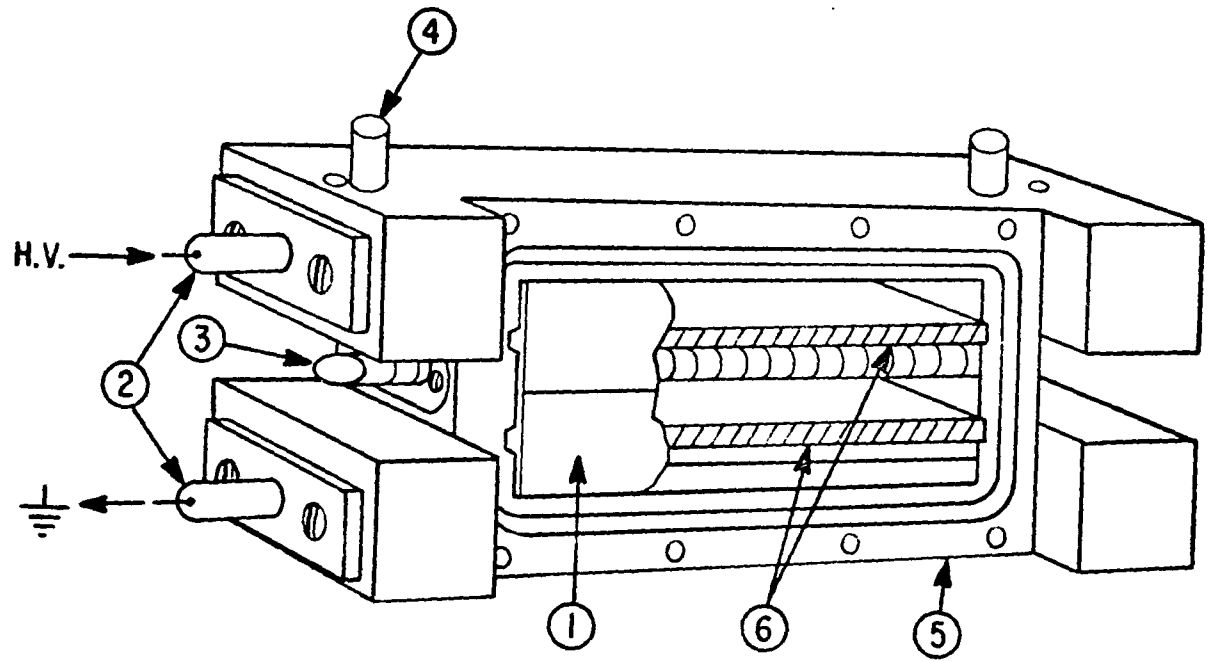
- 4. OFF AXIS 1.06 μ m MIRROR
- 5. 85 % 1.35 μ m MIRROR
- 6. OUTPUT BEAM

Figure 3.1 General Laser Configuration

stimulated emission is driven by the resulting excited states of the laser material. The radiation oscillates between the mirrors in the cavity and with each oscillation 15% of the radiation is transmitted through the output mirror resulting in the output beam. The micrometer mirror mounts provided for both a horizontal and vertical adjustment.

The mirrors obtained from the Valpey Corporation were deposited on optical glass substrates polished flat to one-tenth wavelength in the visible. One was coated for 99% reflectivity at $1.35\mu\text{m}$ and the other for 85%. Both were to have less than 5% reflectivity at $1.06\mu\text{m}$. Spectrophotometer runs at this laboratory found the reflectance to be closer to 6% and 7%. Consequently, considerable difficulty was experienced with unwanted lasing at $1.06\mu\text{m}$ throughout the course of the laser development.

Details of the laser head are shown in Figure 3.2. The samarium glass shields protect the laser material from ultraviolet damage and also offer some protection to the rod in the event of flashlamp breakage. The flashlamps, laser rod, and side plate of the laser head were all mounted with O-rings to provide a water tight seal. The flashlamps extend through the laser head and are electrically connected in series on the side of the head not shown. A water circulation unit provided a constant flow of water through



- | | |
|---------------------------|-----------------------------|
| 1 SILVER PLATED REFLECTOR | 4 WATER CIRCULATION PORT |
| 2 FLASHLAMP | 5 SIDE PLATE REMOVED |
| 3 LASER MATERIAL | 6 SAMARIUM GLASS UV SHIELDS |

Figure 3.2 Laser Head Details

the laser head to dissipate the heat from the flashlamps. The laser head temperature varied from 25°C to 40°C depending on the firing frequency of the flashlamps. Unless otherwise indicated, wavelength measurements were carried out in this temperature range. The circulation unit also had a thermostatically controlled heater to vary the water temperature from room temperature to near the boiling point. The flashlamps were energized by a 100 μ f capacitor bank that could be charged up to 3000 volts. The laser rod was 3-1/4 inches long by 1/4 inch in diameter with the ends cut and finished at the Brewster angle.

The laser was initially set up with a 99% reflecting 1.06 μ m mirror and a 45% reflecting 1.06 μ m mirror as the output coupler. This allowed for an easier checkout as neodymium doped materials will readily lase at 1.06 μ m. After the laser was properly aligned and lasing, the 1.06 μ m mirrors were replaced with the 1.35 μ m mirrors. The wavelength region of the output radiation was determined by checking for penetration through 99% reflecting 1.06 μ m or 1.35 μ m mirrors placed in the laser beam. Beam detection was accomplished by simply checking the emulsion burn on an unexposed polaroid print. The color of the burn against the black background of the print gave an indication as to the energy output of the laser, a white pattern indicating the higher energy as most

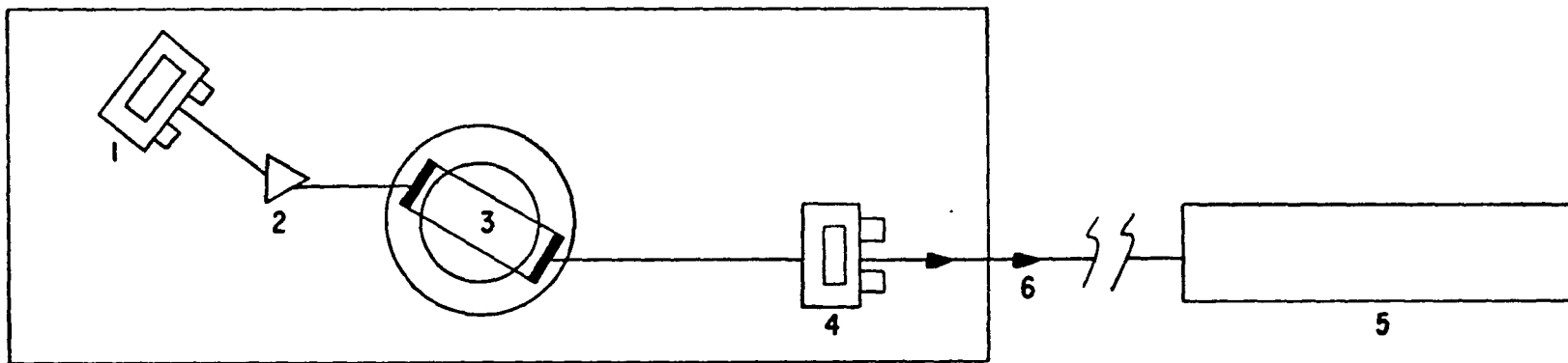
of the emulsion was removed. The shape of the burn was a good indication of proper laser alignment as only proper alignment gives a uniform elliptical burn pattern. The burn pattern is elliptical because the laser rod is skewed at the Brewster angle. No burns could be made through a 99% $1.06\mu\text{m}$ mirror and it therefore became apparent that none of the lasing was at $1.35\mu\text{m}$. The upper lasing level in neodymium is common to both the $1.06\mu\text{m}$ and the $1.35\mu\text{m}$ transition; hence the $1.06\mu\text{m}$ transition must be stopped in order to obtain lasing at the desired $1.35\mu\text{m}$.

The lasing at $1.06\mu\text{m}$ could be quenched by placing a 99% $1.06\mu\text{m}$ mirror off-axis in the cavity (space between mirrors where lasing oscillations occur). This off-axis mirror was then brought close to alignment incrementally while the flashlamps were fired at their maximum rating. This method failed to produce any lasing at $1.35\mu\text{m}$ and when the $1.06\mu\text{m}$ mirror reached alignment the laser would lase from it. No different Nd:glass was available at that time and it was necessary to try other neodymium-doped laser materials. The two other materials available were neodymium doped yttrium orthoaluminate (YAlO_3) commonly referred to as YALO, and neodymium doped yttrium aluminum garnet, referred to as YAG.

The Nd:YALO and Nd:YAG Laser

The first of these new materials to be tested was a Nd:YALO rod, manufactured by Union Carbide, serial number 075. With the $1.35\mu\text{m}$ mirrors, this material readily lased in the $1.3\mu\text{m}$ region without an off-axis $1.06\mu\text{m}$ mirror in the cavity. A Jarrell-Ash half-meter Ebert Spectrometer was used to determine the wavelength, which was measured as $1.3414\mu\text{m}$. The linewidth appeared to be less than 1\AA which might be expected since YALO is a crystalline substance and all of the neodymium atoms see essentially the same field. Thus, it appeared that this particular Nd:YALO rod would not work as its wavelength did not match any of the HF lines. However, other materials cited in the literature has lasing lines close to one of the levels of HF.

Smith (1968) reported a Nd:YAG line at $1.319\mu\text{m}$. Since this closely matched the P(4) level of HF, the laser was reassembled with a YAG rod. This laser material would only lase at $1.06\mu\text{m}$ in the existing configuration. However, by returning the off-axis $1.06\mu\text{m}$ mirror to the cavity, the lasing converted to the $1.3\mu\text{m}$ region. The wavelength of this line was measured to be $1.3380\mu\text{m}$. To obtain lasing on the line of interest, a Brewster prism was introduced into the cavity as shown in Figure 3.3. An article by Bloom (1963) helped in determining the proper angles to



1. 99% 1.35 μm MIRROR

2. PRISM

3. LASER HEAD

4. 85% 1.35 μm MIRROR

5. HELIUM-NEON ALIGNMENT LASER

6. LASER BEAM

Figure 3.3 Laser Configuration with A Prism in the Cavity

align the laser. Dispersion of the prism was approximately 3° per μm at $1.35\mu\text{m}$. In this configuration, the dispersion of the prism prevents lasing at $1.06\mu\text{m}$ and an off-axis $1.06\mu\text{m}$ mirror is not required. With the prism in the cavity, lasing could only be obtained on one of the several possible Nd:YAG lines and the wavelength was determined to be $1.3190\mu\text{m}$. At this time it was noted that the P(4) level of HF as reported by Mann et al. (1961) was apparently not sequenced the same as the adjacent levels. Further checking and reference to the work at Herget et al. (1962) proved that the P(4) transition has a wavelength of $1.3212\mu\text{m}$. The incorrect value as reported by Mann was the inadvertent permutation of two numbers in the reported value of the level in wave numbers, 7586.62cm^{-1} versus the correct value of 7568.62cm^{-1} . This corrected value of the P(4) level did not match the wavelength found in the YAG laser and it was realized that other materials or techniques would have to be tried.

A second Nd:YALO rod, serial number 038, was placed in the laser head with the prism in the cavity. There were two lasing lines found in this configuration. The first had a wavelength of $1.3394\mu\text{m}$, and the second, which was much weaker than the first, had a wavelength of $1.4020\mu\text{m}$. A third Nd:YALO rod was then tried, serial number P47, and

it would only lase on one line, the wavelength of which was determined to be $1.3392\mu\text{m}$.

Table 3.2 summarizes the wavelength of the materials tested along with the closest levels of HF. The linewidths of both the Nd:YAG and the Nd:YALO are narrow and none of the wavelengths were close enough to the HF levels to pump directly. Another material was available, $\text{Nd:LaNa}(\text{MoO}_4)_2$. This material, although crystalline, is much like glass in its spectral width and should exhibit a line of sufficient width to match one or more of the HF levels. The characteristics of this material were studied by Morozov et al. (1966). Again, this material would only lase at $1.06\mu\text{m}$. An off-axis mirror was placed in the cavity in an attempt to switch the lasing to the $1.3\mu\text{m}$ region. The flashlamps were fired at their rated capacity and at that point lasing was obtained at $1.06\mu\text{m}$ from the output coupler and one end of the laser rod, since this rod had the ends finished at 90° to the rod axis. Another off-axis mirror was placed in the cavity to prevent the rod end lasing, in which configuration the system would not lase at all.

Wavelength versus Temperature Dependence of YALO

At this point it was realized that some method would have to be found to shift the narrow lasing lines of the neodymium-crystal lasers available. Returning to another literature search, it was found that Kushida (1969)

TABLE 3.2

SUMMARY OF THE WAVELENGTHS MEASURED
FOR THE VARIOUS LASERS TESTED

Material	Wavelength (air)* of the material	Wavelength (vacuum) of nearest HF level
	μm	μm
YAG	1.3190	P(4) - 1.3212
YAG	1.3380	
YALO-P47	1.3392	P(6) - 1.3404
YALO-038	1.3394	
YALO-075	1.3414	
YALO-038	1.4020	P(11) - 1.3999

* $\lambda(\text{vacuum}) \approx \lambda(\text{air}) + .0004 \mu\text{m}$

investigated the thermal shifts and linewidths of Nd:YAG from 4.2°K to 500°K. Almost all lines shifted to longer wavelengths and broadened with increasing temperature. Although he only investigated the transitions resulting in the 0.94 μ m and the 1.06 μ m regions, it was thought that if similar effects occurred in the 1.34 μ m region, then one of the Nd:YALO lines might be shifted to match the P(6) level of HF.

The Nd:YALO rod, serial number 038, was again placed in the laser head and wavelength measurements were made as the temperature of the circulating water was increased from 22°C to 94°C. During the first run a small decrease in wavelength was noted, although the signal detected at the spectrometer was weak at the higher temperature. Since this run was not conclusive, a new grating was obtained for the spectrometer that was ruled at 590 grooves per mm. and was blazed for 1.35 μ m. This replacement improved the resolution by a factor of two and increased the signal strength. Another run was made heating the water to 94°C. Again, no significant shift in wavelength was noted and it was decided to try higher temperatures. The water was removed from the laser head, which was then wrapped with heating tape. The temperature of the laser head was then monitored by means of a thermocouple temperature probe placed inside the head through one of the water ports.

The wavelength versus the temperature was checked up to 110°C. Wavelength shifts of up to 6Å were observed with no apparent pattern. During the second such high temperature run it was noted that the wavelength seemed to shift with the flashlamp firing. After two more unsuccessful attempts to obtain a wavelength versus temperature dependence, the heating tape was removed and the laser head was reconnected to the water circulation unit. The water temperature was again varied and it was apparent that the spectral properties of the YALO rod had undergone a significant change. The resulting wavelength versus temperature curve is shown in Figure 3.4 and, as of now, this effect is still unexplained. Results of a different nature were obtained by Weber and Varitimos (1971) who measured the fluorescence spectrum of Nd:YALO from 77° to 300°K. Their results in the region of 1.34μm show line broadening, but very little or no line shift. The results obtained here for Nd:YALO 038 were unique. Subsequent runs demonstrated a similar cyclic pattern in wavelength with a period varying from 27°C to 35°C. Also, the peak points in the wavelength do not necessarily remain at the same temperature. Several more runs were made to verify that the laser could be temperature tuned to the desired wavelength and it was found that the wavelength 1.3400μm could be approached from either above or below in temperature on either of the three regions

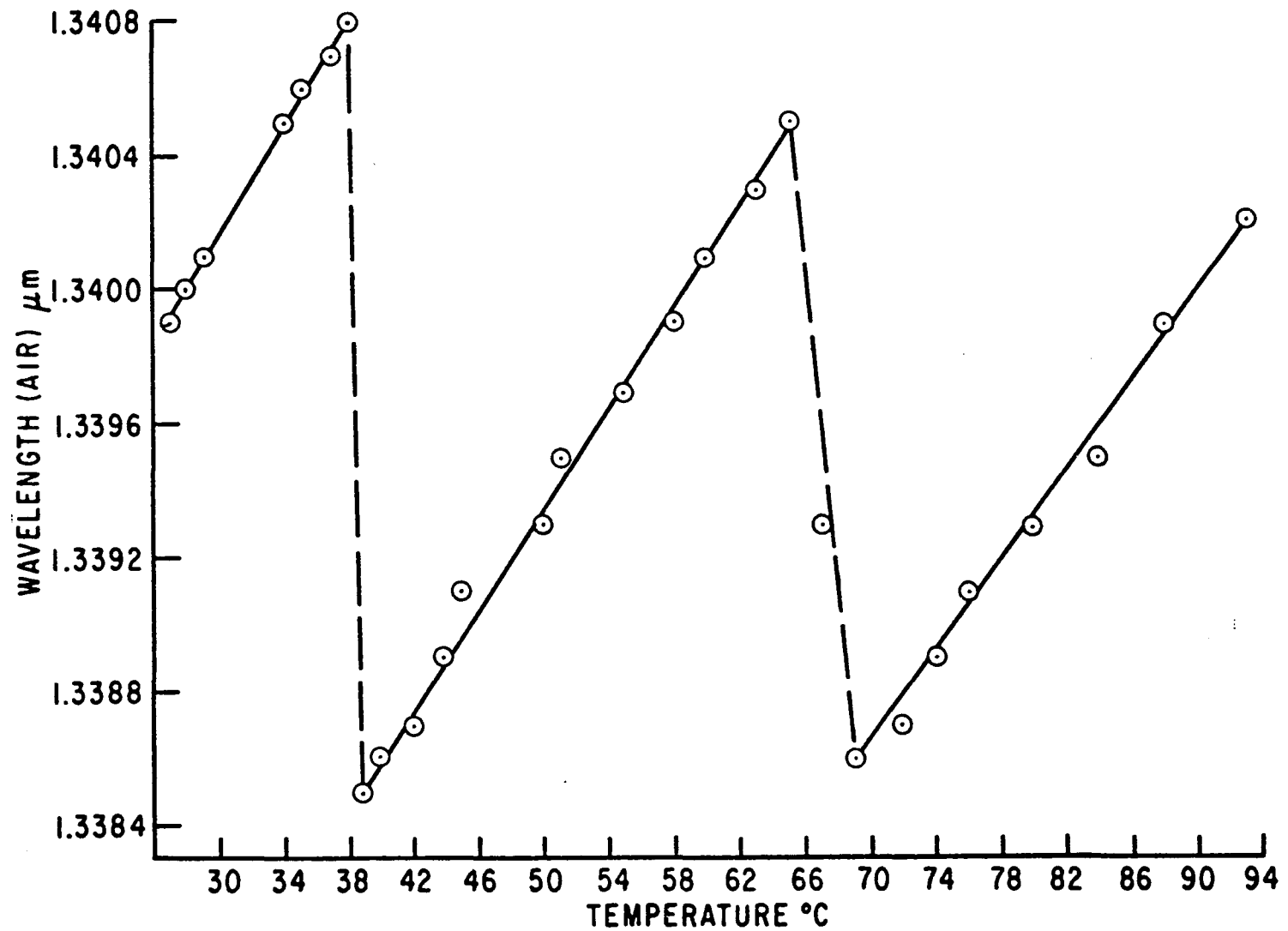


Figure 3.4 Wavelength Versus Temperature for Nd:YALO 038

available on the curve. This wavelength, λ (air) = 1.3400 μm matches that of the P(6) level of HF. (Note that there is nearly a 4\AA difference between the value as measured in air and vacuum.)

With a laser available that was tunable to one of the HF levels, preparations were made to attempt pumping of the second vibration level. There were still experimental difficulties associated with the operation of the laser. Perhaps the most serious problem was that the alignment of the laser varied with temperature which affected the output energy. This necessitated periodic adjustment of the mirrors and, on occasion, after such an adjustment it was found that the wavelength had reverted back to the bottom of the curve. Hence, by the time the laser was tuned to the proper wavelength, it was often operating at a fairly high temperature. The higher temperature accentuated another of the experimental difficulties of the laser, that of corrosion of the silver reflector. The water circulating in the system was distilled and deionized and was changed periodically. Several types of plastic and rubber connecting tubes were tried to determine whether the plasticizers were responsible for the corrosion. A gold-plated reflector was tried, but it was unacceptable as it reduced the efficiency too much below that found for silver. Consequently, the laser head had to be opened to clean and polish the silver

reflector every two to four days depending on the operating temperature.

In an attempt to excite the second vibrational level of HF, the laser was tuned to a point just below the proper wavelength and fired into the HF cell while the temperature was increased in small steps until the wavelength had passed that of the HF level sought. No fluorescence was observed and it was assumed that the energy of the laser was insufficient. Energy measurements of the laser output were made using a thermopile. Figure 3.5 shows a typical slope efficiency curve for YALO 038. The typical energy per pulse was approximately 70 millijoules. The calculations shown in Appendix D indicated that the energy was at the lower limit and, since no fluorescence was observed, it was decided that it would be necessary to increase the amount of energy delivered to the cell.

Energy Enhancement Techniques

The first attempt at increasing the pumping energy was Q-switching. This does not actually increase the energy output of the laser, but simply delivers all of the energy in one pulse over a very short period of time. Typically, during the long pulse mode of operation, the energy is delivered in approximately 50 to 100 μ sec. Figure 3.6 shows a typical long pulse from the YALO laser as detected by

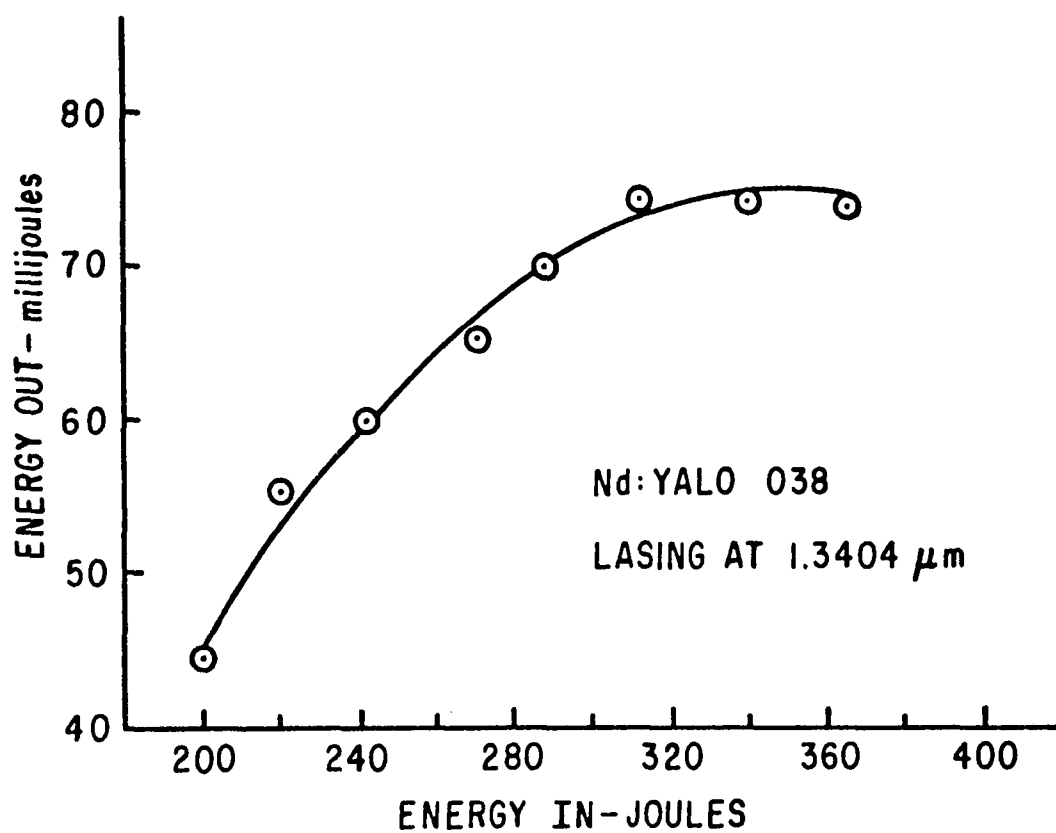


Figure 3.5 Slope Efficiency Curve for YALO 038

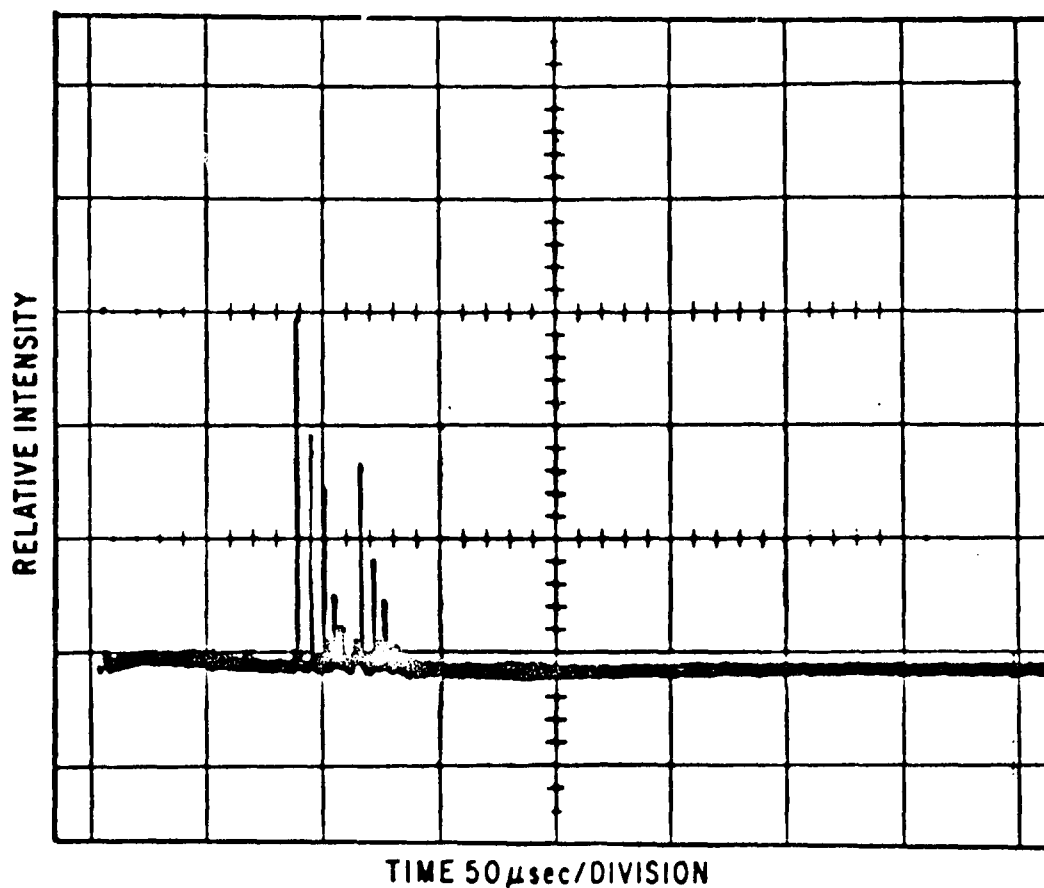


Figure 3.6 A Typical Long Pulse Mode of the Nd:YALO Laser

the germanium detector on the spectrometer. The purpose of Q-switching in this case is to avoid the energy dilution with time so that, when pumping occurs, all of the fluorescence generated will take place in one very short period of time. Even if the relaxation of the excited HF is slow enough so that cumulative pumping takes place during the long pulse, the Q-switched pulse should give a better fluorescence trace from a data reduction standpoint.

The circuitry used for Q-switching is shown in Figure 3.7. The variable phase pulser was adjusted such that its output pulse would trigger the flashlamps at the proper time prior to rotating prism alignment. To fire the laser, the fire switch was depressed which then passed the variable phase pulse to an amplifier. The amplifier output caused the SCR (silicon controlled rectifier) to provide closure for the 300 VDC to actuate the flashlamp trigger. The rotating prism assembly was manufactured by Hadron and had a speed capability up to 600 cycles per second. Since the rotating prism was totally reflecting and offered no wavelength selectivity, an off-axis $1.06\mu\text{m}$ mirror had to be used in the cavity. Wavelength selection was then only afforded by the 85% $1.35\mu\text{m}$ output mirror. Later, another Q-switching unit was obtained from Hadron that would accept the standard one inch diameter 99% $1.35\mu\text{m}$ mirror. This eliminated the need for the off-axis $1.06\mu\text{m}$ mirror.

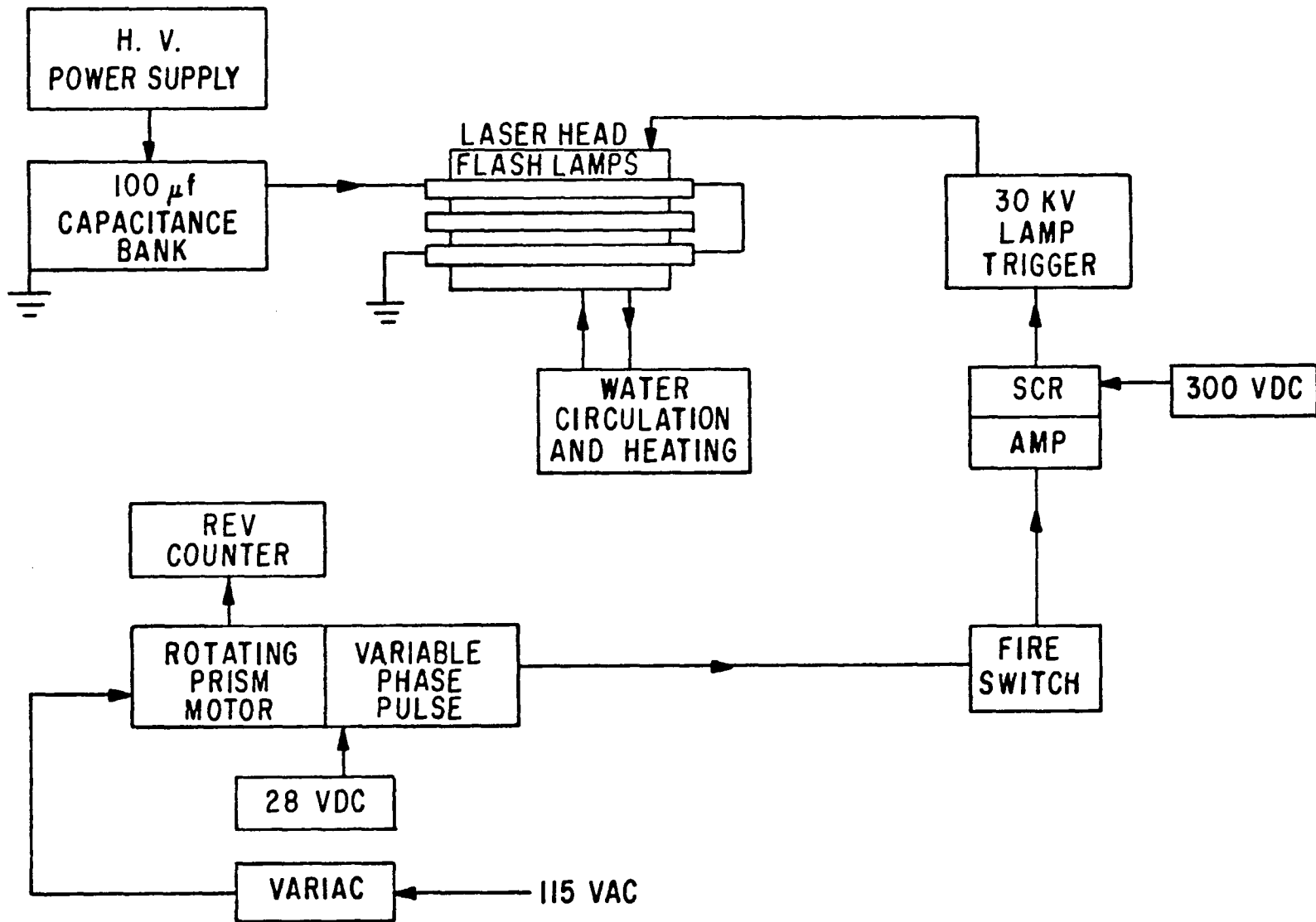


Figure 3.7 Q Switch Circuit

Operation of the laser in the Q-switched mode while varying the wavelength with the temperature was always difficult. It was found that the best operation was at low rotational speeds. Early operation was at 200 cycles per second and this was later reduced to as low as 75 cycles per second with no signs of post lasing (one or more lasing pulses occurring after the main pulse is normally referred to as post lasing). The main difficulty with Q-switching was due to an effect mentioned earlier, that of the wavelength changing with alignment as the mirror rotated. Also, after showing the wavelength-temperature dependence for approximately 11 weeks, the laser at this point began to lase at two wavelengths simultaneously. One of the wavelengths was $1.3394\mu\text{m}$, the original wavelength that the YALO rod displayed prior to the temperature dependence effect, and the other was at a value that followed the temperature curve. However, the laser would Q-switch at $1.3394\mu\text{m}$ most of the time. Figure 3.8 shows the results of a complete temperature cycle with and without Q-switching. As can be seen from the plot, the laser would Q-switch at the proper wavelength at only one temperature and it was not reliable at that point. Some other means of energy enhancement had to be found.

Before leaving the subject of Q-switching, another interesting aspect of this laser should be mentioned.

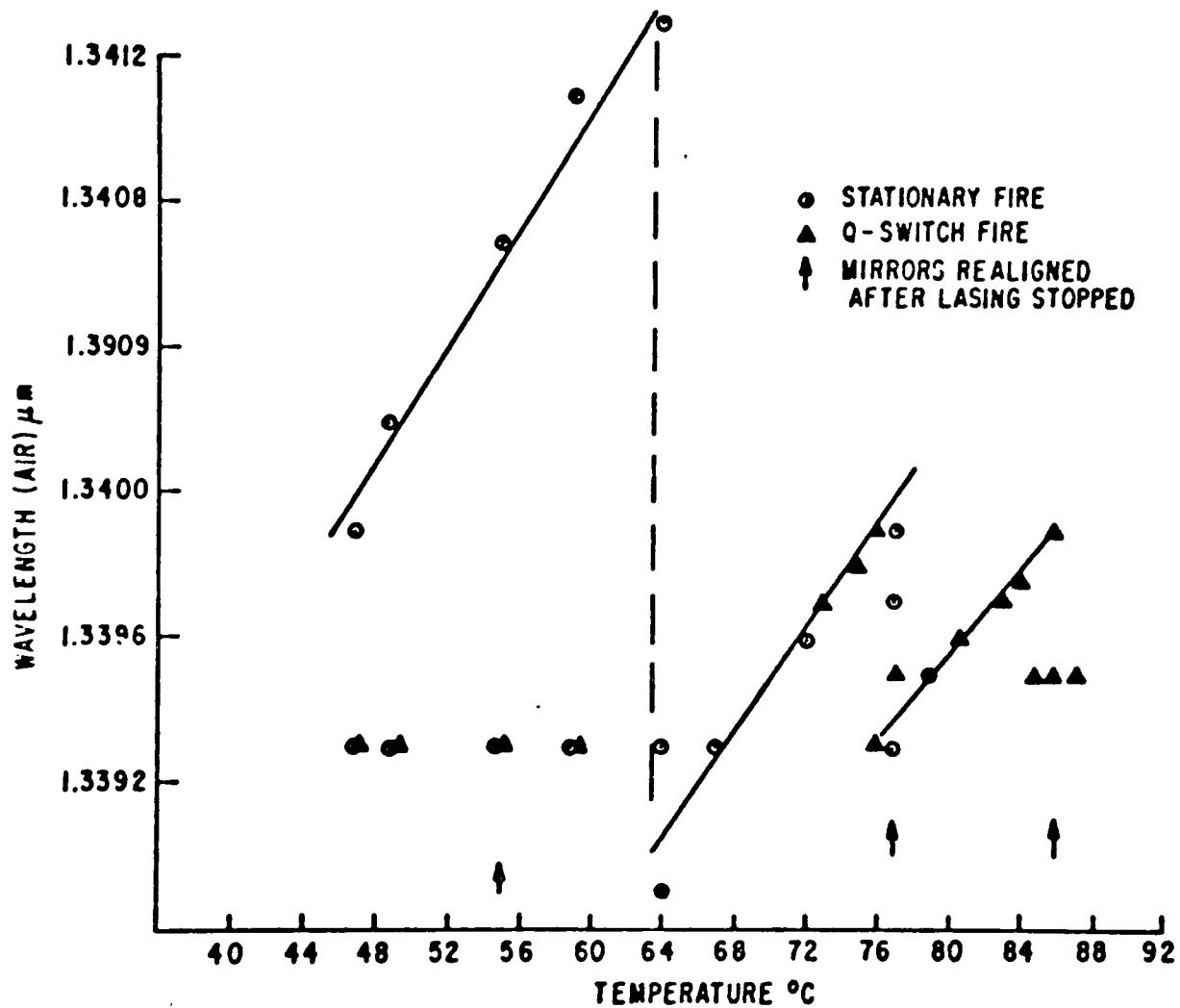


Figure 3.8 Wavelength Versus Temperature with and Without Q Switching

There were times when the laser was fired in the long pulse mode and all of the energy was delivered in a single pulse instead of in the normal multitude of random spikes. At first, attempts were made to find a correlation with the operating point on the temperature dependence curve. However, it was later noted that it lased in this manner just prior to the point at which lasing became difficult, at which time it was necessary to clean and polish the silver reflector. This effect was probably due to operation near the threshold of lasing. As lasing became more difficult to achieve, the flashlamps were fired at increasingly higher voltages. At near maximum voltage, for a given capacitance-inductance combination, the flashlamp pulse became very short compared to its normal value. At a certain point, the only pumping the rod received from the flashlamps above its threshold for lasing was delivered over a very short period of time and all of the lasing occurred in one pulse. The other two YALO rods did not display this effect to the extent that YALO rod 038 with the anomalous wavelength versus temperature effect did.

The final attempt at increasing the energy delivered to the HF cell was made by placing the cell in the laser cavity. Since the output coupler was 85% reflecting, approximately six times as much energy should be available inside the cavity as compared to the output. This assumes no reflection

losses from the cell windows, which had to be placed slightly off-axis to prevent lasing at $1.06\mu\text{m}$. The laser displayed results similar to those obtained during Q-switched operation. Figure 3.9 shows a plot of one such run. The laser did work well on several occasions and, based on measurements on the energy output through the 85% μm mirror, the estimated energy delivered to the cell was as high as 230 millijoules. There was still no evidence of any fluorescence from the HF cell even though supporting calculations indicated adequate energy. Of the several reasons for possible nonpumping that were being considered, the first to be checked was the wavelength match of the laser to the HF.

An experiment was set up to check on the absorption of the laser pulse as it passed through the HF cell. Quartz beam splitters were placed before and after beam passage through the HF cell to direct small portions of the beam into germanium detectors. The signals from the detectors were sent into a dual beam oscilloscope where their intensities were balanced with no HF in the cell. The cell was filled with HF at a pressure of 500 torr to obtain some pressure broadening and to improve absorption. The temperature of the laser was then varied from below to above that which gave the correct calculated wavelength for absorption. The results of this experiment are shown in Figure 3.10. It was proven that the wavelength of the laser

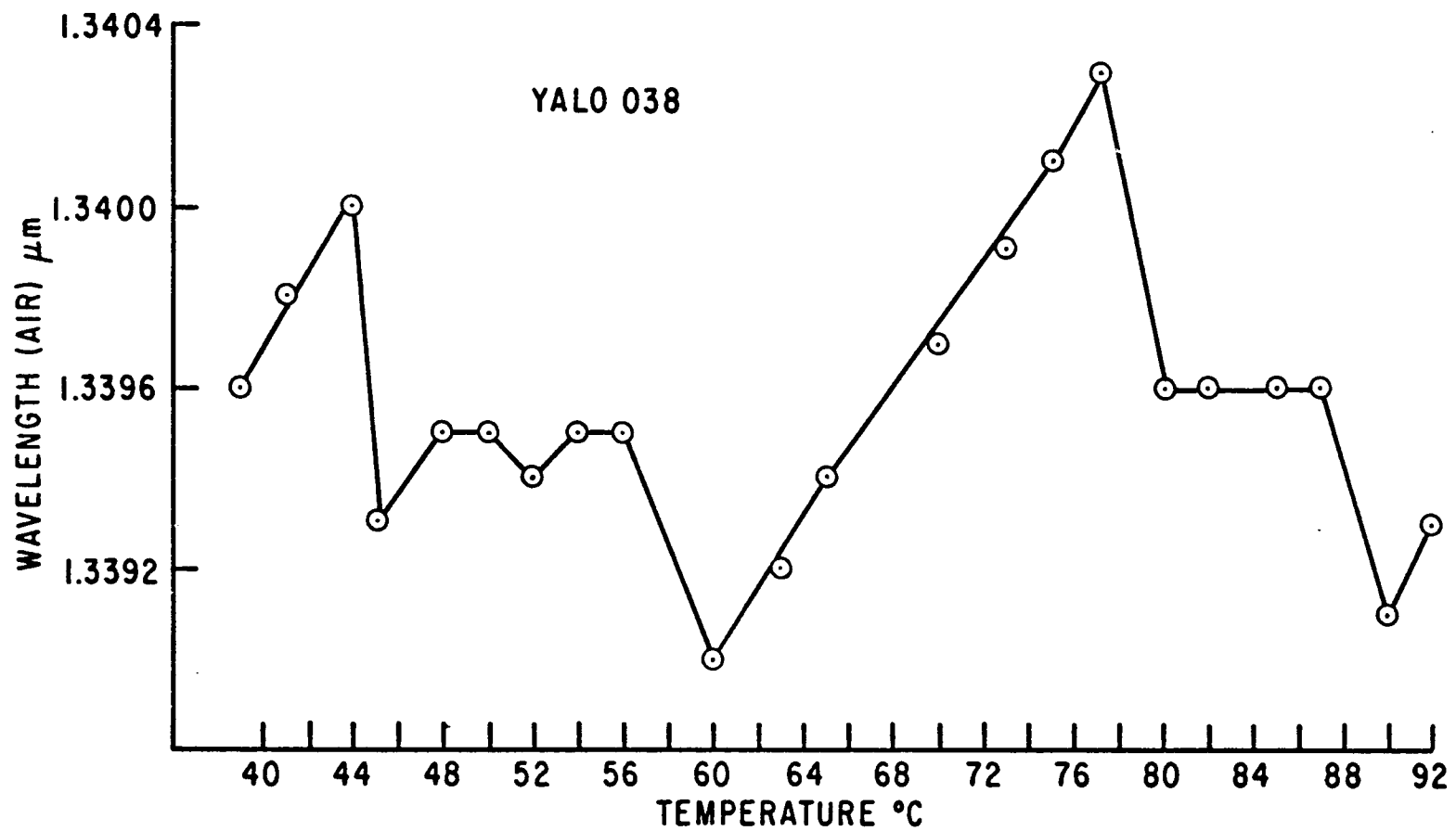


Figure 3.9 Wavelength Versus Temperature with the HF Cell in the Cavity

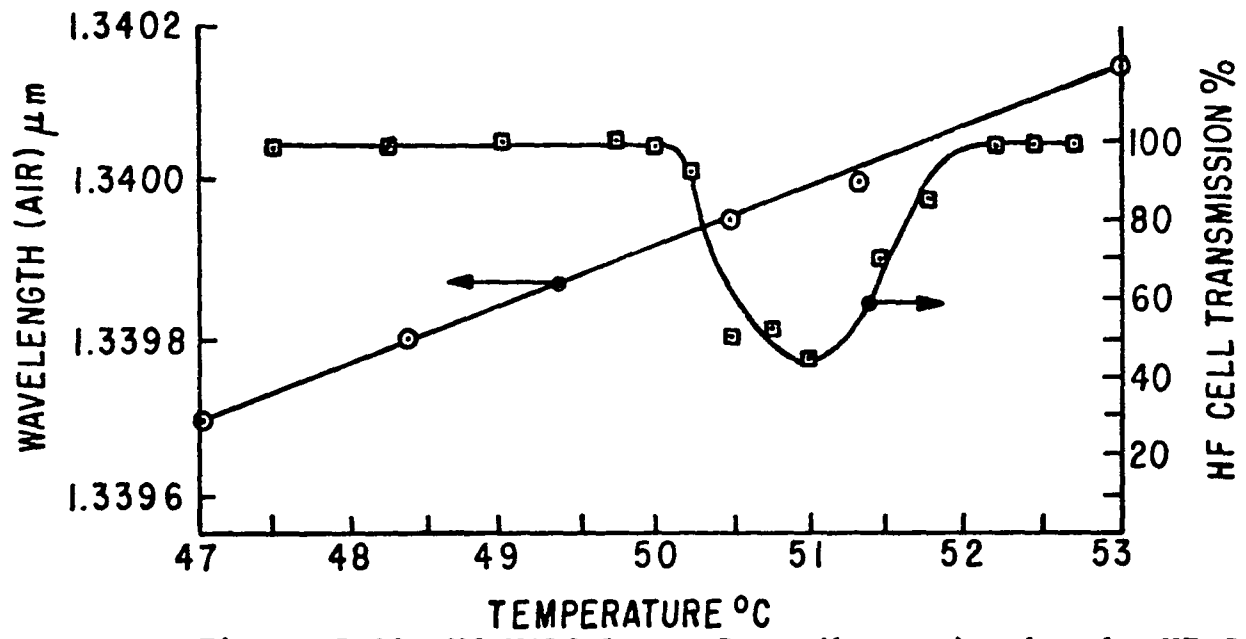


Figure 3.10 Nd:YALO Laser Beam Absorption by the HF Cell

could be matched to that of the ($V=0 \rightarrow 2$) P(6) level in HF. This reduced the reason for nonpumping to the only portion of the system left unchecked at this time, the HF cell mixture and the IR detector assembly.

At this point it was shown that the reason for non-pumping was the lack of an adequate HF mixture in the cell. Details of the HF gas handling problems and how they were solved can be found in Appendix A. When this problem was eliminated, the YALO laser in its normal configuration was able to excite the second vibrational level of HF on two occasions. It was not necessary to Q-switch or have the cell in the laser cavity in order to pump the HF.

Pumping was not achieved again and the difficulty was shown to be that the wavelength versus temperature dependence was beginning to deteriorate. Figure 3.11 shows a plot where the wavelength increases with temperature for only one cycle. Note that the desired wavelength of $1.3400\mu\text{m}$ is obtained only in the vicinity of 71°C and that the rod is not well controlled at that point. The laser head was disassembled and the YALO rod was placed in a furnace and taken to 110°C and then allowed to cool slowly. This restored the wavelength-temperature dependence of the rod, but a full examination of the results was not possible due to an unfortunate loss of the laser. A flashlamp failure, which led to steam generation inside the laser head,

destroyed the entire head assembly, including the YALO rod that demonstrated the desired wavelength-temperature dependence.

An effort was made to induce a change in YALO rod P47 similar to that which had occurred in YALO rod 038 giving it the wavelength versus temperature dependence. Repeated thermal cycling of the rod did not induce the desired change. This rod did, however, show linear wavelength versus temperature response that could possibly lead to lasing at $1.3400\ \mu\text{m}$. Figure 3.12 shows the results of the thermal cycling of the rod. The slope of the curve was decreasing, and the temperature of the rod required to obtain lasing at $1.3400\ \mu\text{m}$ was getting to be very high. Lasing at these high temperatures was very difficult and the signals were just strong enough to operate the spectrometer. If this material was to work as a laser to pump the second vibrational level of HF, there would have to be a considerable developmental effort required.

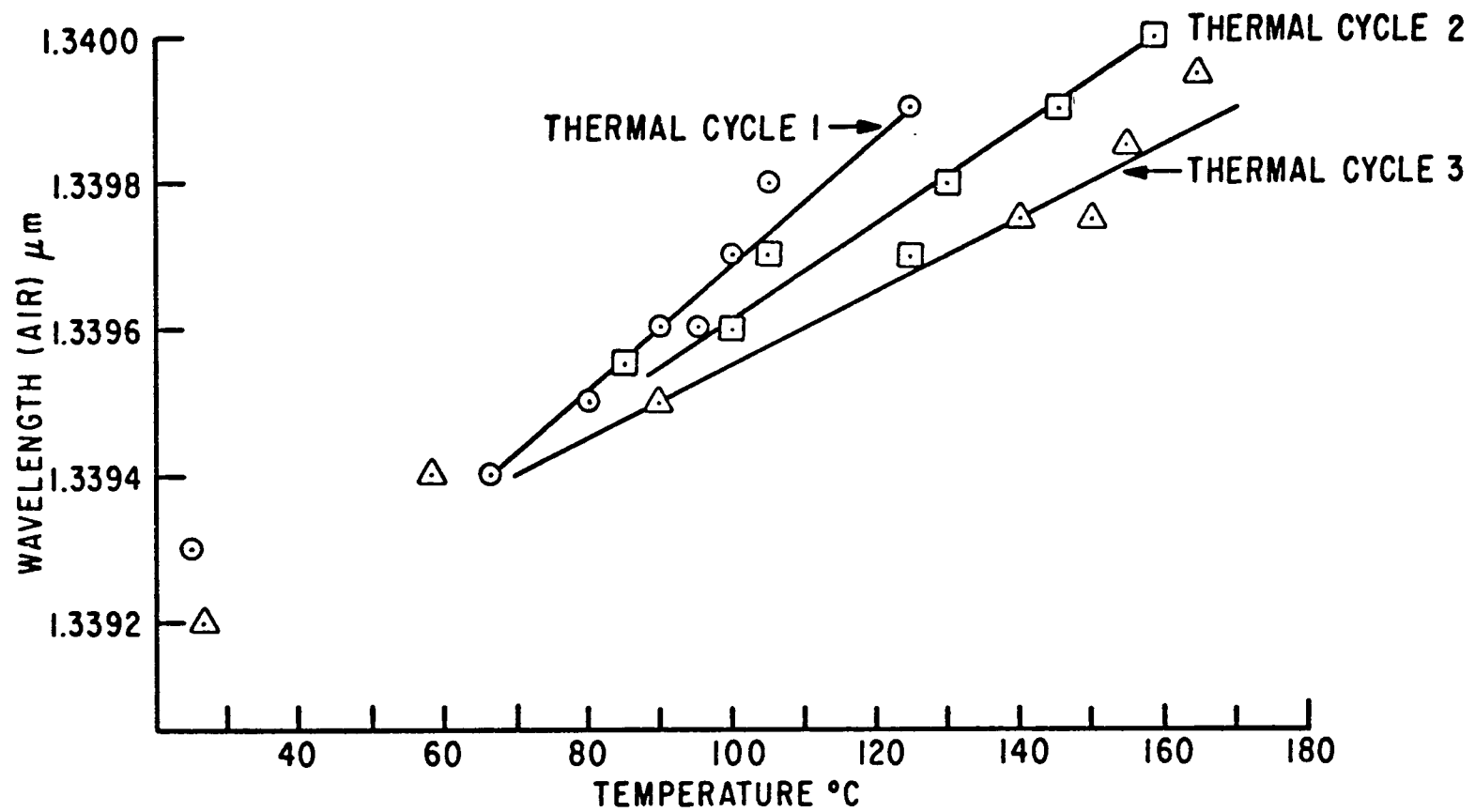


Figure 3.12 Wavelength Versus Temperature for Nd:YALO P47

CHAPTER 4

EXPERIMENTAL TECHNIQUES

The purpose of this chapter is to describe the overall operation of the equipment used in this experiment. While the development of the YALO laser used in excitation of the HF was covered in Chapter 3, this discussion will be directed toward specific operating procedures. Similarly, details of the gas handling system, the HF pin laser, and the infrared detector assembly are covered in the appendices. The operation and interplay of these systems shall be discussed in more detail here. The overall experimental arrangement is shown in Figure 4.1.

The starting point of any run was to establish a flow of an HF-Ar mixture through the test cell at a fixed pressure. Pressures were varied from 5 torr to 30 torr. The HF gas handling system had a 20 liter stainless steel mix tank which contained a prepared mixture of HF in Ar. Mixtures used were either a 5% or 2% mixture of HF in Ar at a total tank pressure of about 800 torr. Details of the gas handling system, including a gas purification and mixing procedures, can be found in Appendix A. A gas flow was established from the mix tank into the test cell and on into a mechanical pump. The

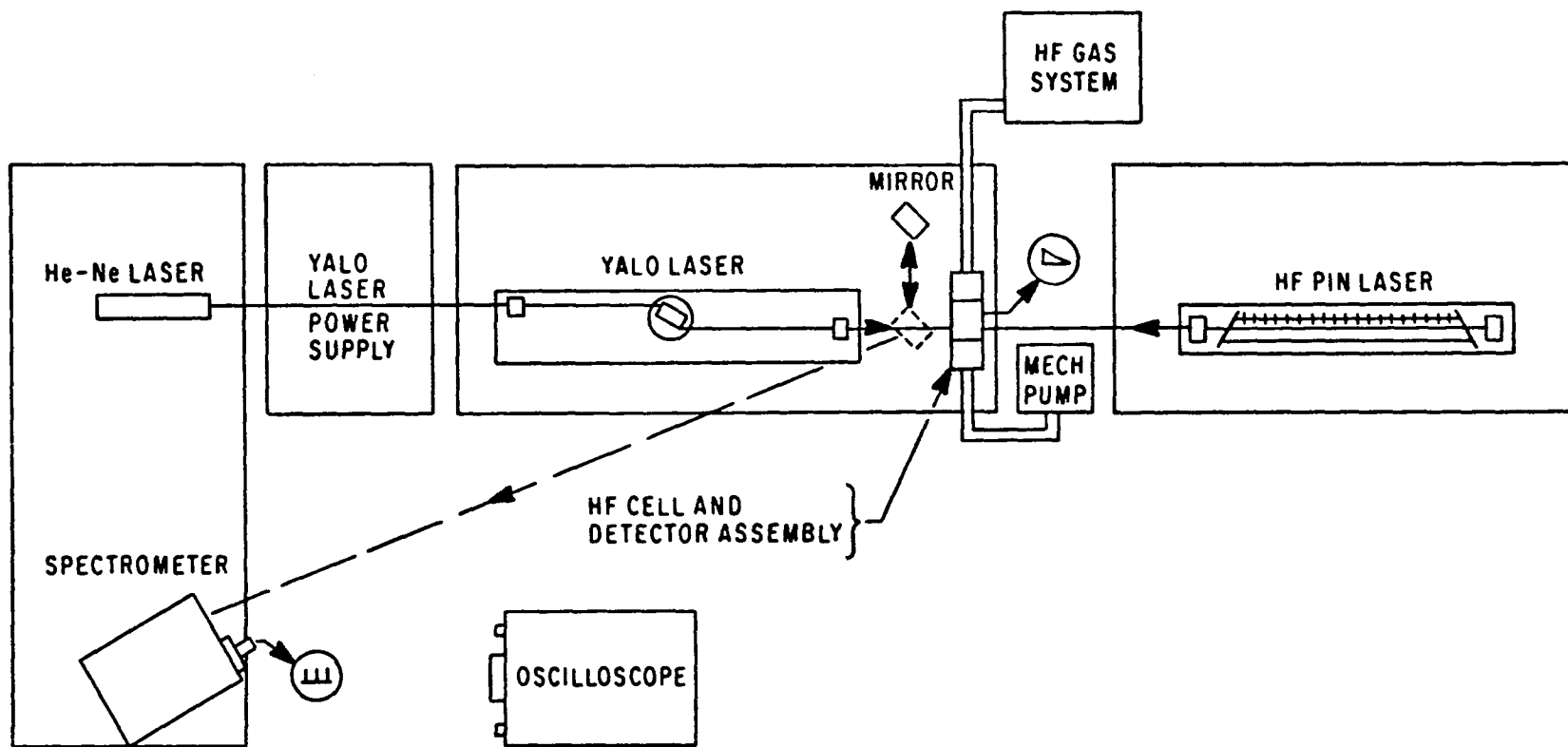


Figure 4.1 Experimental Arrangement

pump exhaust was discharged into a high volume laboratory hood. The gas flow was regulated by throttling valves on both sides of the cell. The pressure was measured just downstream of the cell by an all-stainless-steel strain-gauge pressure transducer.

Hydrogen fluoride gas has properties that require the use of special handling techniques. In addition to being highly reactive chemically, HF has the property of readily adhering to surfaces. Airey and Fried (1971) have reported on many of the problems encountered when handling HF. Quantities of HF will adhere to the vacuum-baked walls of a test cell and its associated plumbing. Following a decrease in pressure, this HF is again readily liberated. With sufficient time, equilibrium will be established in a constant pressure flow, and the amount of HF being adsorbed on or leaving the walls will approach zero. This condition is referred to as passivation. It should be noted that the term passivation as referred to in the literature often implies a surface fluoride formation. In any system both a chemical reaction at the wall surface and adsorption will take place. The important reaction for any particular system will depend on the volume to surface ratio. In large volume to surface ratio systems, such as shock tubes, adsorption is a lesser problem.

Cell passivation time varies according to what HF partial pressure the cell has been exposed to prior to initiating the flow. Initial passivation of the cell after a new mixture has been prepared can take several hours because portions of the lines leading to the mix tank have been exposed to 100% HF during the preparation of the mixture. Wall exposure to these high concentrations of HF results in heavy surface absorption and in wall outgasing during the initial flow. Once these lines have been cleared of the excess HF, small changes in the partial pressure of HF required considerably less time to passivate.

Cell passivation was considered complete when consistent values of P_{τ} could be obtained for the same values of the measured total pressure. Since an accurate partial pressure was not easily obtained in this experiment by conventional means, the partial pressure of HF in the cell was determined by measuring the relaxation time, τ , and calculating the pressure based on the accepted value of P_{τ} . Measurements made after the cell was sufficiently passivated gave values of P_{τ} , based on pressure readings of the transducer, that agreed within 10% of the accepted values. However, during the short periods of time that the YALO laser was operating properly and exciting the HF, there was not sufficient time to allow for passivation following pressure changes. It then became important to find the correct value of the HF partial pressure

by measuring τ . The recent work of Bott (1972) lists the room temperature value of $P_{\tau}(V=1 \rightarrow 0)$ as $17.8 \mu\text{sec-torr}$.

The relaxation time that was used to determine the HF partial pressure was measured by monitoring the fluorescence of the $V=1$ level induced by an HF pin laser. The HF pin laser was used to pump the HF molecules in the test cell into their first vibrationally excited level. The relaxation time was then obtained by photographing the detected fluorescence trace on an oscilloscope camera. The details of this pin laser are presented in Appendix B.

The fluorescence was detected with an indium antimonide (InSb) detector operating at liquid nitrogen temperature. Details concerning the construction of the detector assembly can be found in Appendix C. Signals from the detector were amplified by a low noise 40DB preamplifier before entering the 1A7A preamplifier of a Tektronix 556 oscilloscope. Sweep triggering in the oscilloscope was taken from the incoming signal. A standard polaroid camera attachment on the oscilloscope recorded the fluorescence trace. The relaxation time could then be easily determined directly from the photograph, giving an indication of cell passivation and the partial pressure of HF. The method for determining P_{τ} from the photograph is discussed in Chapter 5.

Once the gas flow had been established and the proper passivation determined by measuring consistent relaxation

times with the pin laser, the YALO laser could be set up for direct excitation of the second vibrational level. The first step in operating the YALO laser was to determine at what wavelength it was operating. To do this a mirror was placed between the laser and the HF cell to fold the beam back into the half-meter spectrometer (see Figure 4.1).

The laser beam was aligned to strike the center of an ordinary piece of white paper covering the entrance slit of the spectrometer. The paper served to present the spectrometer with a diffuse source and to protect the grating from the direct effects of the laser beam. Signal detection at the exit slit of the spectrometer was by means of a Philco-Ford L-4520 germanium detector. This detector was so sensitive that a preamplifier was not required at the detector itself, and the signal was sent directly to the preamplifier of the oscilloscope. The spectrometer had a digital wavelength readout, which for the grating used had a resolution of 1\AA in the first order. As the spectrometer grating was moved incrementally through the wavelength region of the YALO laser's emission, the oscilloscope trace could either be observed visually or photographically. Calibration of the spectrometer dial indicator was accomplished by folding the Helium-Neon laser beam back onto the entrance slit of the spectrometer with another mirror. The calibration was obtained by noting the dial correction factor needed to

obtain the Helium-Neon lasing wavelength of $6328\overset{\circ}{\text{Å}}$. This calibration could only be accomplished by visually observing the exit slit of the spectrometer since the power level of the Helium-Neon laser was not sufficient to activate the detector. Using the spectrometer to monitor the wavelength, the temperature was then varied so as to set the wavelength just below that of the $V(0\rightarrow 2) P(6)$ transition of HF.

The folding mirrors were then removed and the YALO laser could be fired into the HF cell. The laser was fired single shot by means of a capacitor bank that was charged with a variable output high voltage supply, and then discharged through the flashlamps. The discharge through the flashlamps was initiated by means of a 30 KV trigger transformer.

The detection of the infrared fluorescence is identical to the procedure used when operating the HF pin laser. A $2.0\mu\text{m}$ to $3.0\mu\text{m}$ filter was placed directly on the upper cell window to reduce the amount of scattered $1.34\mu\text{m}$ radiation seen by the InSb detector by two orders of magnitude. The oscilloscope traces were observed visually while the YALO laser was fired and the laser temperature increased incrementally to set the wavelength at the proper value for excitation of the HF. When evidence of overtone excitation was observed by means of the fluorescence trace, photographs were taken. Figures 4.2 and 4.3 show typical photographs of

traces obtained from YALO laser pulses that in the case of Figure 4.2, resulted in no excitation and in the case of Figure 4.3, caused direct excitation of the second vibrational level. In both of these photos the laser was operating in the single pulse mode. Figure 4.4 shows an oscilloscope photograph of a YALO laser pulse, firing the long pulse mode, that is particularly interesting because only one of the individual pulses associated with the laser firing was on the proper wavelength for excitation of the HF.

The typical fluorescence traces shown in Figures 4.3 and 4.4 were taken from the two instances when excitation of the second vibrational level was successfully achieved in this experiment. In the first case, Figure 4.3, when the laser was operating in the single pulse mode, five photographs were taken that contained good quality fluorescence traces. During the second instance, Figure 4.4 with the laser operating in the long pulse mode, two photographs were obtained.

The conditions necessary for excitation of the second vibrational level were proper wavelength, adequate energy, a proper gas mixture in the cell, and a detector sensitive enough to monitor the fluorescence. The last two items were readily checked by using the HF pin laser to excite the first vibrational level in the cell and observing the fluorescence. The wavelength could be measured with the spectrometer and

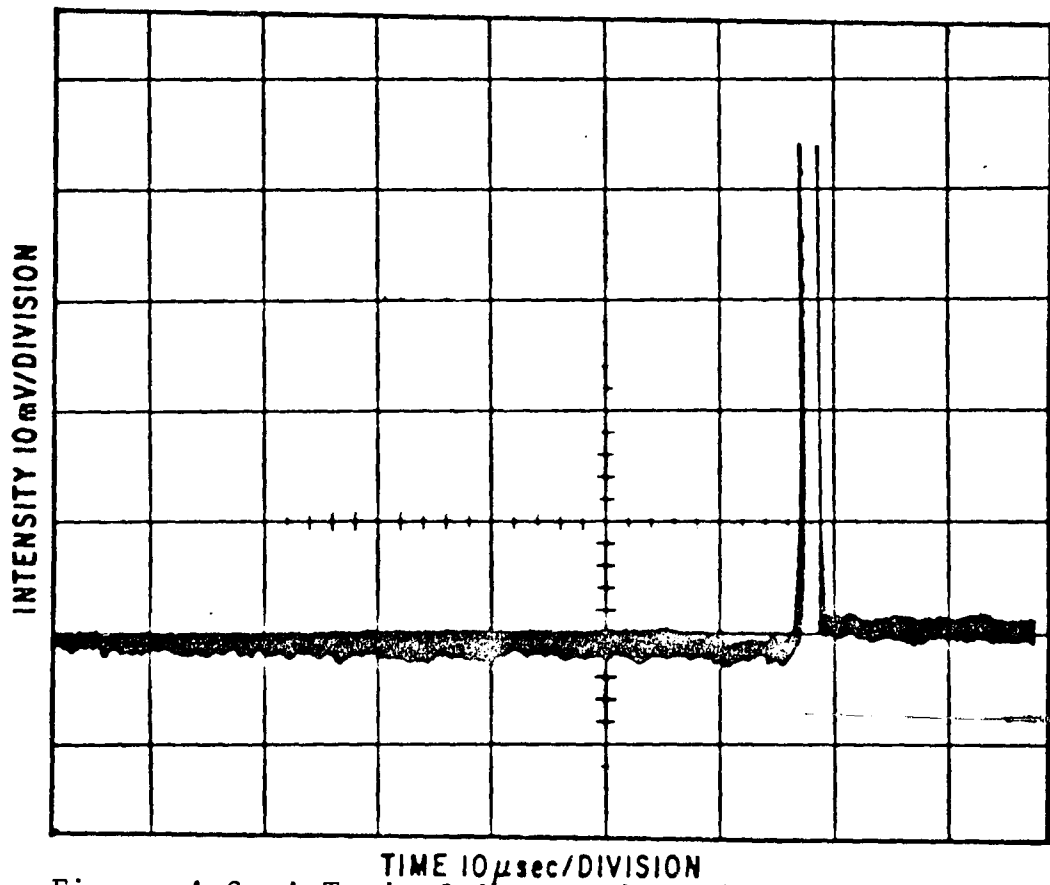


Figure 4.2 A Typical Nonpumping Nd:YALO Laser Pulse,
Operating in the Single Pulse Mode

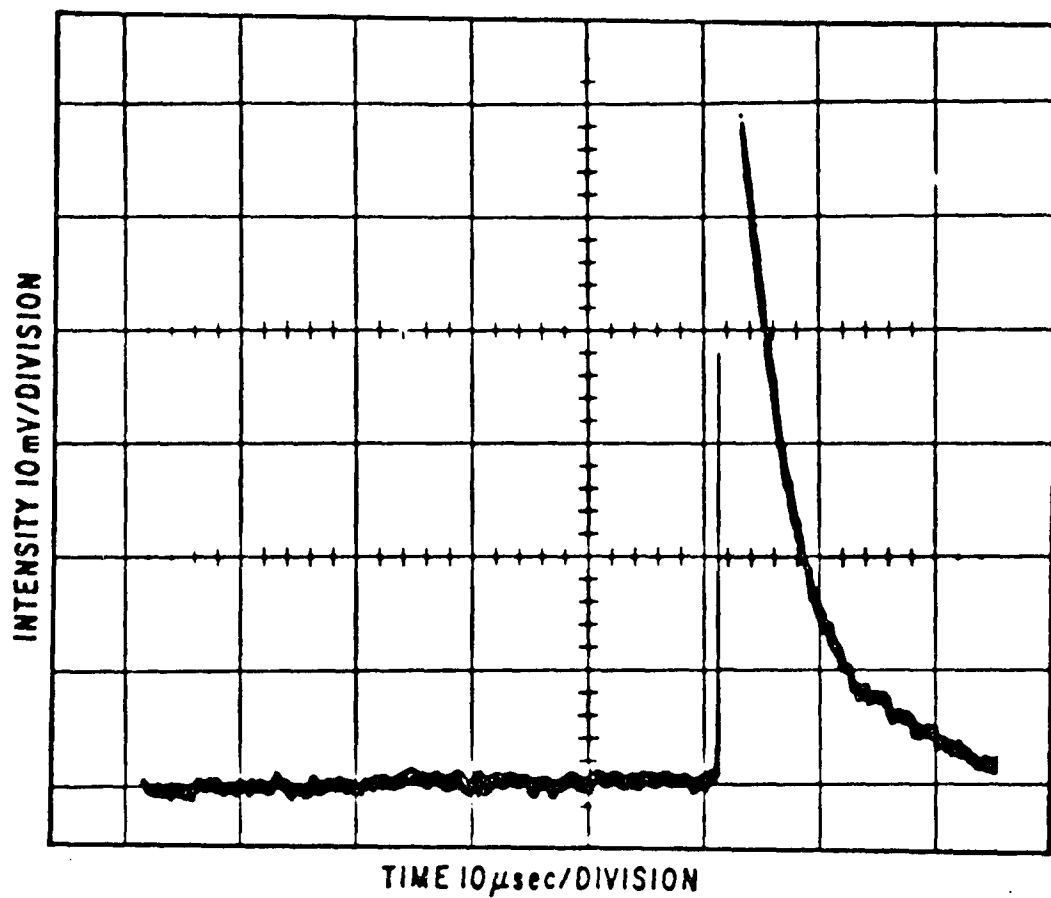


Figure 4.3 A Typical Pumping Nd:YALO Laser Pulse,
Operating in the Single Pulse Mode

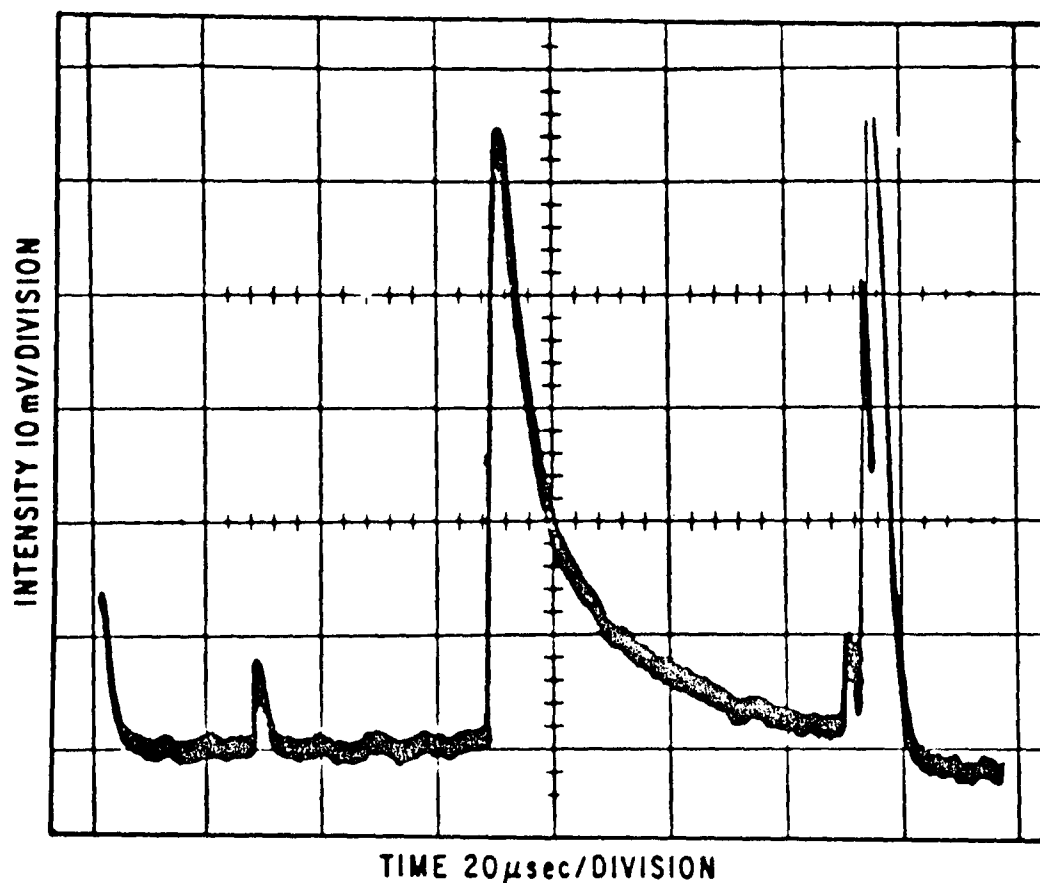


Figure 4.4 Trace 8-2A a Pumping YALO 038 Pulse,
Laser in the Long Pulse Mode

the energy level set at or above that which had been proved to be adequate earlier. There were, however, many times when all conditions were apparently correct for excitation of the HF, but none was observed. The exact reason for this has not been completely resolved, although it is most probably due to a wavelength mismatch. This explanation is supported by the photograph shown in Figure 4.4 that shows only one of the pulses of the long pulse mode exciting the second vibrational level. This would indicate that the wavelength match was critical since the wavelength shift during one firing of the laser should be very small. On the other hand, spectrometer measurements of the spectral width of the YALO laser indicate a half maximum full width on the order of 1\AA . Maximum instrument broadening of the spectrometer, as determined by observing the width of the Helium-Neon laser line which is less than 0.1\AA , was on the order of 0.5\AA . The spectrometer was used in the second order when measuring the linewidth of the Helium-Neon laser, thus the measurement of the broadening was good to 0.5\AA . Thus, the non-excitation of the HF by the YALO laser in some cases is supported by some of the evidence and contradicted by others. In both cases when excitation of the second vibrational level was achieved the wavelength was measured at the expected value of $1.3400\mu\text{m}$.

The photographs obtained by the methods described in this chapter constitute the raw data of this experiment. The

means by which these photographs were analyzed are described in the next chapter.

CHAPTER 5

RESULTS AND CONCLUSIONS

Experimental results of the measurement of the deactivation rate of the second vibrational level of HF are presented in this chapter. The data obtained in this experiment consisted of photographs of oscilloscope traces showing the decay of fluorescence intensity with time. The method by which relaxation times were determined from these photographs, and how parameters such as the partial pressure of HF and the associated electronics effected the data is discussed. After the results are presented, the last section of this chapter discusses the conclusions and recommendations for future work.

Data Interpretation and Results

After excitation by the laser pulse, the fluorescence intensity decreases exponentially with time, with the time constant associated with this exponential decay being a measure of the relaxation rate of the fluorescing species. In the determination of this time constant, a plot is made of the natural logarithm of the fluorescence intensity versus time, a procedure which results in a straight line. The relaxation time is then obtained directly from these straight-line plots. Therefore, data reduction in this experiment was a process of

obtaining plots from the photographs and then determining the slopes.

The data points for the plots were obtained by overlapping the photographs with a narrow-spaced grid on a light box and reading the points from the oscilloscope trace. These points were then plotted on semi-logarithmic graph paper. Figure 5.1 is a representative plot showing the results for trace 8-2A. The photograph of oscilloscope trace 8-2A was shown in Figure 4.4. Each plot resulted in two straight lines as a result of the double exponential decay of the HF(V=2) species. Initially, all of the excited HF molecules are in the V=2 level because of the selective resonance pumping of the excitation laser. The fluorescence observed is the result of these molecules cascading to their ground vibrational level, probably in the sequence (V=2→1) and (V=1→0). The relaxation (V=2→1) is probably some combination of (V-V) and (V-R-T) processes. Thus, the first exponential is the relaxation of the V=2 level and the second exponential is the relaxation of V=1 level.

Straight lines were fitted to the data points and the slopes in the line, γ_2 and γ_1 , were determined. As discussed in Chapter 2, the relaxation time, τ , for each mode of decay is the reciprocal of the slope characteristic of that part of the decay curve. The relaxation associated with the (V=2→1)

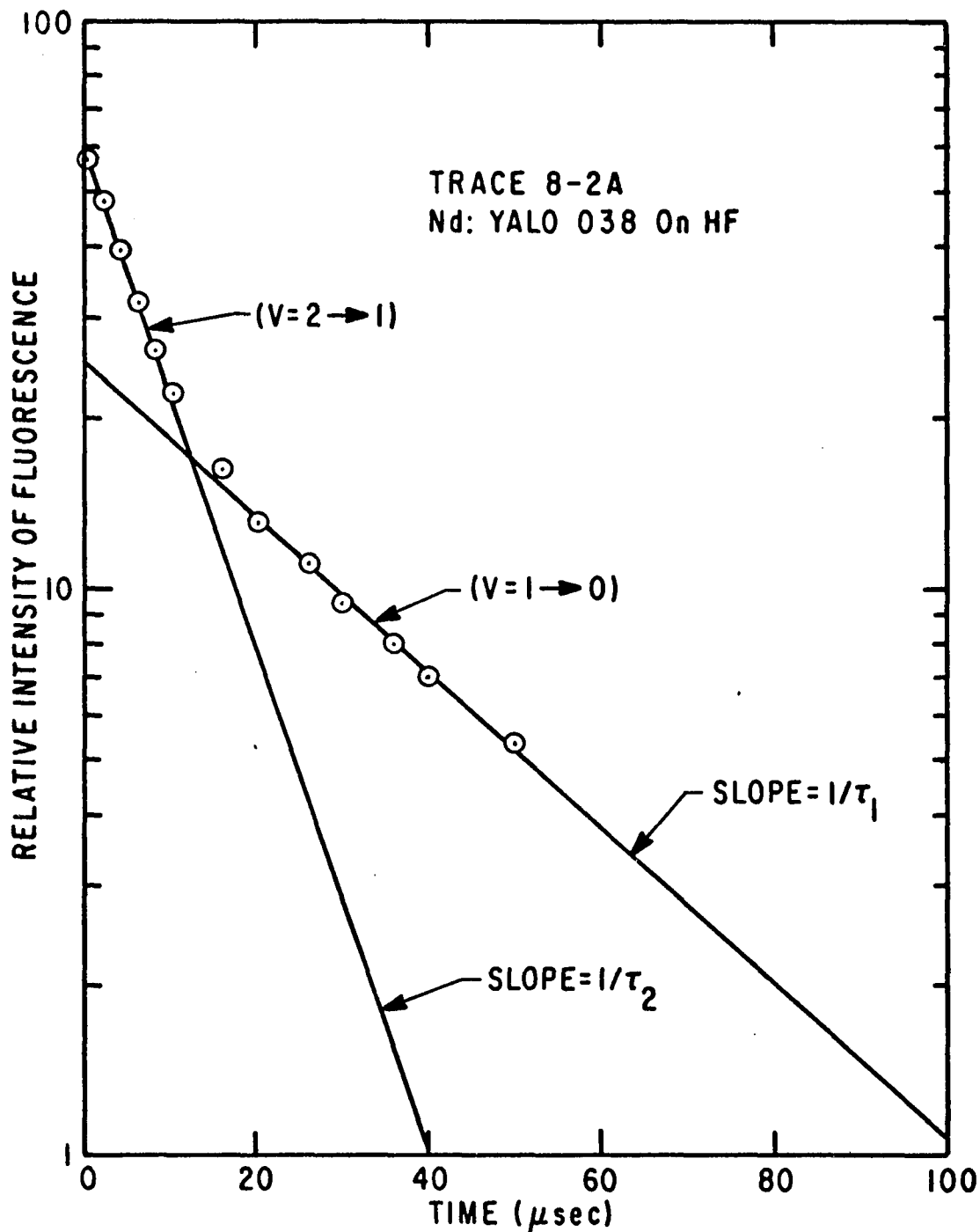


Figure 5.1 A Semi-log Plot of the Data Points from an Oscilloscope Trace Showing the Double Exponential. $T = 300^\circ\text{K}$

decay is designated at τ_2 , and the relaxation of the second exponential decay, ($V=1 \rightarrow 0$), is designated as τ_1 .

In order to determine P_τ , the partial pressure, P , of the HF in the mixture must be known in addition to the measured relaxation time, τ . The partial pressure of HF for each set of conditions was determined from the HF($V=1 \rightarrow 0$) relaxation time measured by means of the HF pin laser. As discussed in Chapter 4, the partial pressure is obtained from the relaxation time by using the recently obtained room temperature value of $P_\tau(V=1 \rightarrow 0) = 17.8 \mu\text{sec-torr}$. Bott (1972) has consistently obtained this value of P_τ and values within 10% of his measurement were obtained in this work after sufficient time had elapsed at one pressure to ensure passivation of the HF cell. The long passivation time required to reach a steady-state pressure of HF in the cell corresponding to the gauge indication precluded simply using the pressure read directly from the gauge. Values of the product of the partial pressure and the relaxation time, P_τ , were then obtained for each of the two slopes taken from the plots. The results are tabulated in Table 5.1.

Included in Table 5.1 are the average values of P_{τ_1} and P_{τ_2} . As can be seen, there is a 21% variance with the value reported by Bott (1972). However, Fried, Wilson, and Taylor have recently found values of P_τ for HF($V=1$) at a temperature of 350°K that vary from 10.6 $\mu\text{sec-torr}$ to 22.8 $\mu\text{sec-torr}$. Thus, there are still experimental discrepancies

TABLE 5.1

RELAXATION TIMES OBTAINED FROM THE EXCITATION
OF THE SECOND VIBRATIONAL LEVEL OF HF AT 300°K

Trace No.	$P\tau_1$ μsec-torr	$P\tau_2$ μsec-torr	τ_1/τ_2
5 - 30M	16.0	9.50	1.68
8 - 30M	12.9	5.34	2.41
9 - 30M	16.3	6.37	2.56
13 - 30M	13.7	5.66	2.42
17 - 30M	14.3	8.47	1.69
8 - 2A	11.6	4.14	2.79
9 - 2A	12.6	6.86	1.84
<p>Average $P\tau_1$ = 13.9 μsec-torr Average $P\tau_2$ = 6.62 μsec-torr Average τ_1/τ_2 = 2.20 ± .42</p>			

to be accounted for in the measurement of the $V=1$ level of HF, which are probably associated with the adsorption of HF on cell surfaces. It is perhaps significant that the results of Bott have the smallest reported error. This suggests that there is less of a passivation problem in a large volume-to-surface ratio shock tube system such as he uses.

As can be seen from Table 5.1, there is considerable scatter in the values of P_{τ_1} and P_{τ_2} . There were several reasons for this. The most significant reason for the scatter was probably due to the inaccuracies in measuring the partial pressure of HF. An attempt had been made to obtain the relaxation time at several values of the total pressure of the HF mixture. This resulted in a non-steady-state HF partial pressure in the cell for most of the data since the time between pressure changes had been inadequate for complete passivation. This problem was alleviated, with a penalty in accuracy, by using the HF pin laser to measure the existing HF partial pressure.

The second problem that caused scatter in the data was associated with the electronics of the detector system. The problem is illustrated in Figure 4.4 wherein the fluorescence trace drops below the base line of the original oscilloscope trace. It was noted that the amount that the trace dropped below the base line, undershoot, was a function of the intensity of the exciting laser pulse as well as the intensity

of the fluorescence produced. The undershoot of the oscilloscope trace resulted in a requirement to establish a new base line prior to analyzing the data from the trace. This new base line, which somewhat affected the value of the relaxation time, was taken to be the minimum value of the trace.

Unfortunately, the problem that caused this undershoot was not discovered until after the data had been taken. The problem resulted from excessive capacitance in the oscilloscope input circuit. This capacitance caused the signal to undershoot following high intensity pulses. After the cause of the electronics problem was discovered, tests showed that relaxation times with and without the capacitive filtering action were different by as much as a factor of 1.5. Since this factor varied with intensity, it was decided that no attempt would be made to correct the data, since there was no quantitative way to determine the peak intensity of the fluorescence on each photograph.

Also listed in Table 2.1 is the ratio of the relaxation time τ_1/τ_2 . Since this ratio is independent of the partial pressure of HF, it is a more significant result than the individual values of $P\tau$. Also, it is believed that the electronic base line shift has little effect on the decay-time ratio τ_1/τ_2 of each trace.

The average value of the ratios, τ_1/τ_2 , is also shown in Table 5.1. As pointed out in Chapter 2, the value

of VP_{τ} has been predicted to be a constant for a harmonic oscillator. Accordingly, for $V=1$ and $V=2$, the relevant HF levels of this work, the ratio should be $(\tau_1/\tau_2)_{th} = 2$. The experimental value of $(\tau_1/\tau_2)_{Avg} = 2.20 \pm .42$ obtained in this work supports this prediction within the uncertainty. The uncertainty reported for the ratio is the standard deviation.

Conclusions

This work was originally undertaken to obtain measurements of the relaxation time of the second vibrational level of HF. The method used, the direct laser induced excitation of the second vibrational level, turned out to be much more difficult than originally anticipated due to the problems involved in the development of the laser itself. However, prior to the accidental loss of the laser, successful excitation of the HF was accomplished on two different occasions with a total of eight successful data points. The data had considerable scatter due to the gas passivation and the electronics problems described above. However, other workers in this field are reporting comparable results. The significance here is in the techniques developed. Now that overtone pumping ($\Delta V > 1$) has been accomplished for the first time, the method will prove to be a powerful tool in measuring the kinetic processes of HF and can be extended to other molecules of interest.

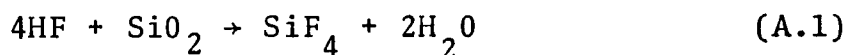
With regard to future work, it is recommended that the larger of the remaining pieces of YALO rod 038, which is approximately 1-1/4 inches long, have the broken end refinished so that more research can be done on its anomalous behavior. As a lasing host, YALO is often referred to as a "poor crystal". This is primarily due to the fact that it damages easily under moderate laser power. However, some of its other properties, such as the possibility of temperature tuning of the wavelength, are definite assets for some applications.

Finally, as mentioned in Chapter 3, the development of YALO rod P47 should be continued. Although it has not demonstrated the wavelength-temperature dependence of YALO 038, it has demonstrated the capability of lasing at the proper wavelength to excite the ($V=0 \rightarrow 2$) level of HF. Operating on that wavelength requires a temperature in excess of 200°C, but the problems associated with the high temperature operation can be solved. Now that the techniques of exciting the second vibrational level has been established, they can be applied to yield many results that were previously unattainable. These will include, in addition to the primary objective of an accurate determination of the relaxation time of the second vibrational level, information such as ($V-V$) rates and possible measurements on rotational equilibrium times.

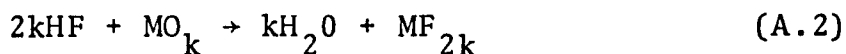
APPENDIX A

THE HYDROGEN FLUORIDE GAS-HANDLING SYSTEM

The hydrogen fluoride gas used in this experiment has several properties which make it difficult to handle. It is highly reactive chemically which requires the use of special materials to store and handle the gas. For example, it reacts with the SiO_2 of glass to form water.



Also, it reacts with metal oxides to form water



where M is a metal atom. It can also react with metals to form hydrogen



The water molecule has many internal degrees of freedom and is therefore an efficient vibrational deactivator of diatomic molecules. In particular, water and HF have many vibrational transitions that are less than one wavenumber

apart, and as a result water is an excellent vibrational deactivator of HF. Consequently, vibrational relaxation measurements made on HF must be done with anhydrous HF and in a system that does not allow the formation of even very small quantities of water.

The generation of hydrogen as an impurity in the HF also presents a problem due to the vibration-to-vibration energy exchange. Airey and Fried (1971) found that this process can lead to vibrational energy sharing between the gases which results in a measured vibrational relaxation time that is considerably larger than that characteristic of hydrogen free HF mixtures.

In addition to the highly reactive chemical nature of HF, it also has the property of readily adhering to surfaces. This was discussed in Chapter 4 in regard to passivation of the system. This property of HF was known, but unfortunately the extent to which HF will be adsorbed on the walls of a test cell was not fully realized. Early attempts to observe fluorescence were attempted using a cell with a static gas fill. It was the negative results obtained using the static cell that led to the addition of the HF pin laser to the experiment. It was found that no fluorescence could be obtained from the cell by using the HF laser. The test cell was disassembled, recleaned and pumped by a diffusion pump with a liquid nitrogen cold trap. It was then leak

tested using a helium leak detector and found to be free of leaks.

Starting with this freshly prepared cell, static mixtures of HF and argon were again made in the cell. At first partial pressures of HF on the order of several torr were tried. After the cell was filled and pumped and then refilled several times, a small fluorescence signal was finally obtained under laser excitation. Suspecting adsorption, the cell was filled with 25 torr of 100% HF, pumped and refilled to a one torr partial pressure of HF. This produced a 15 mv fluorescence signal at the oscilloscope, but after ten minutes the signal was down to 8 mv. As a result of these tests, the HF gas-handling system was set up to operate with a slow steady flow of HF mixture through the cell.

Figure A.1 shows a schematic of the HF gas-handling system. This system is very similar to the systems used successfully by other investigators. All of the plumbing was made of 300-series stainless steel. Figure A.2 shows schematically the construction of HF cell. The cell was made from a solid cube of nickel which was 2-1/2 inches in a side. The four windows (bottom not used) were made of sapphire and and clamped to the cell against Teflon O-rings. An aluminum chassis box supported the cell at the proper level so that both the Nd:YALO and the HF laser beams passed through the

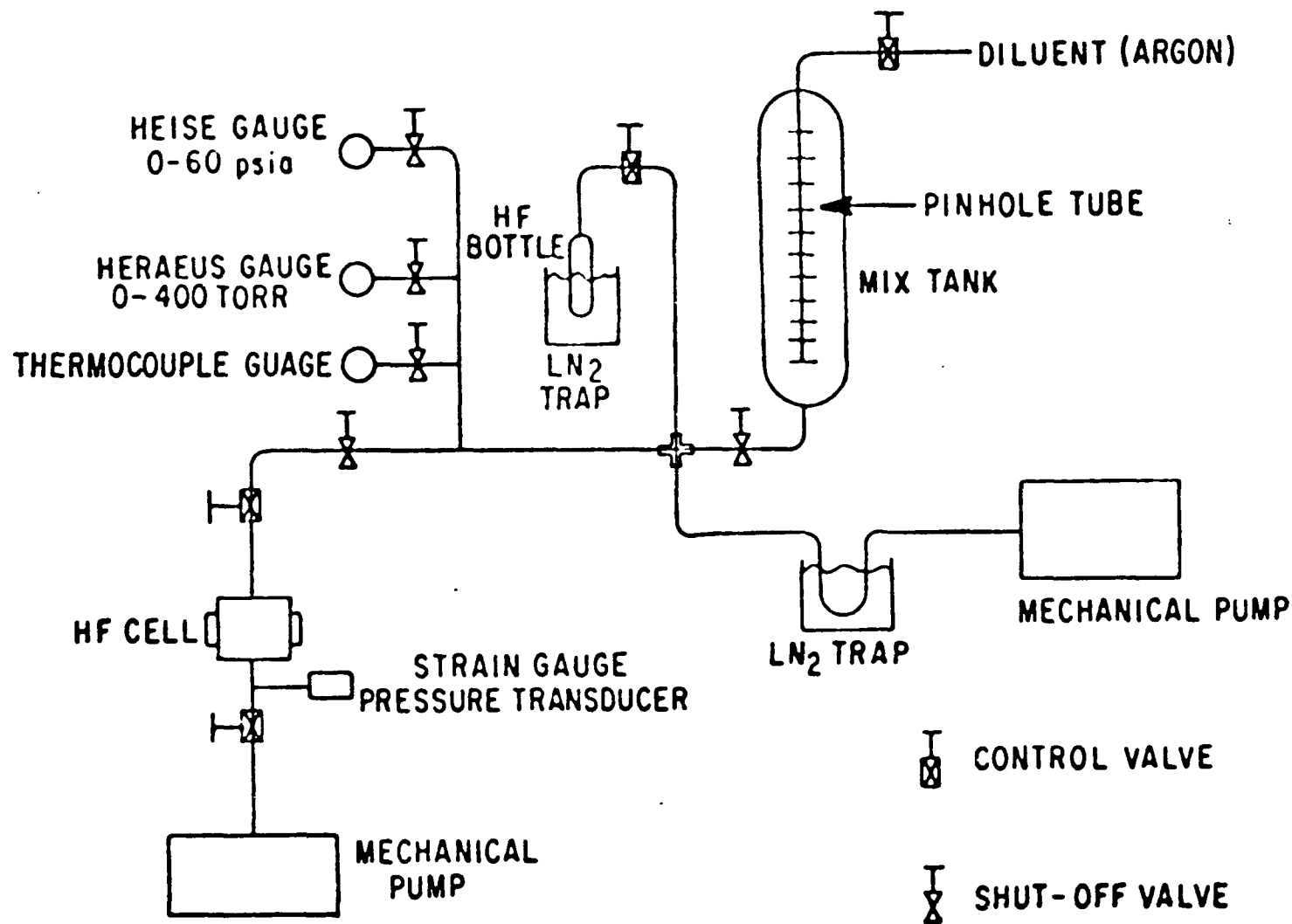


Figure A.1 The HF Gas Handling System

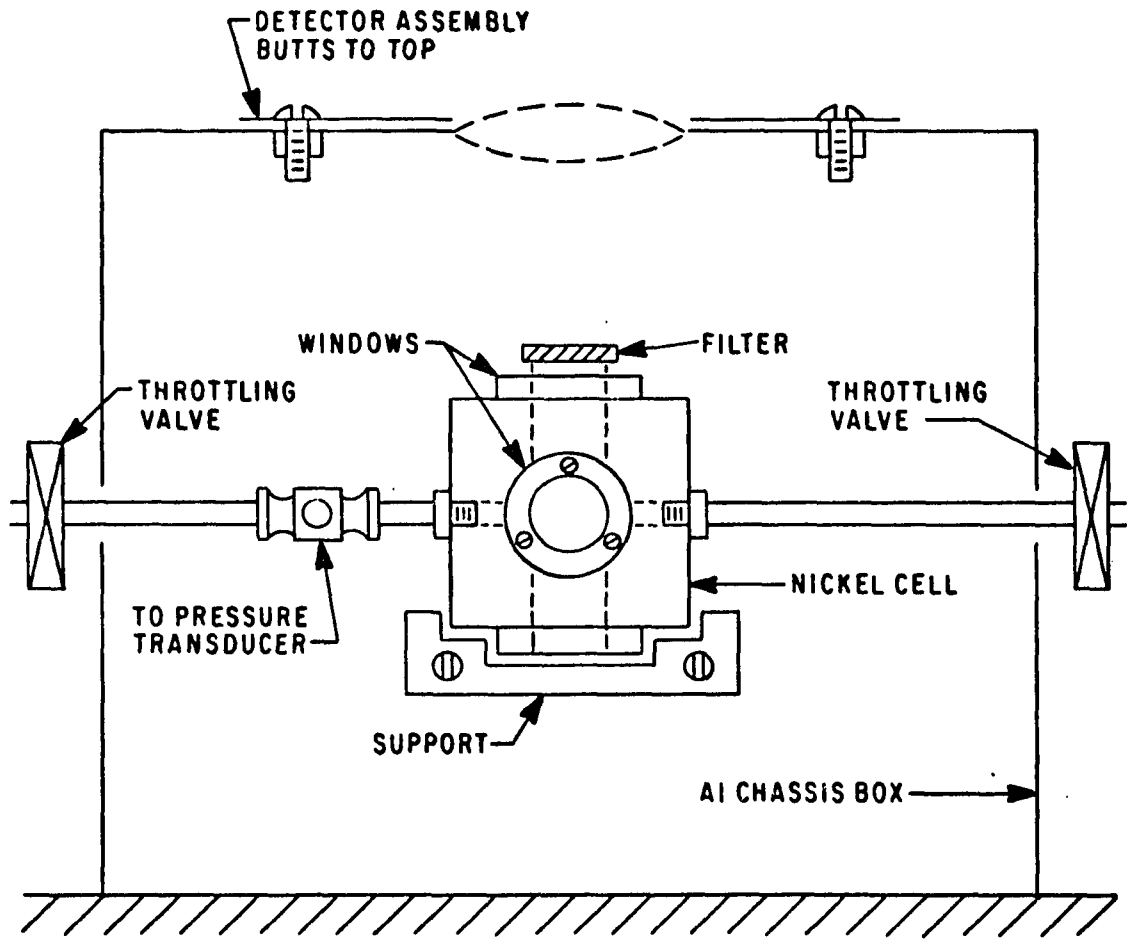


Figure A.2 The HF Cell Assembly

center of the cell. Holes were made in the chassis box and its cover just large enough so as to allow laser beam passage. A filter could be placed directly on the top window of the cell which was located below the light gathering lens of the detector assembly. The detector assembly was fastened directly to the top of the HF cell assembly.

The HF gas used in this experiment was obtained from Matheson and was commercial grade doubly distilled. The first step in preparing a gas mixture was to connect the commercial tank on a stainless steel manifold which contained a stainless steel bottle. This set up was not part of the gas-handling system. After the manifold and bottle were evacuated, the bottle was cooled to liquid nitrogen temperature and then the HF was cryogenically pumped into the bottle. When the bottle was filled with frozen HF it was again opened to the pump to remove any hydrogen. The process was then repeated by transferring this HF to another bottle, except that now the first bottle was only warmed to about -25°C to trap any water.

The bottle containing the HF was then transferred to the HF gas-handling system. At this point the bottle was again frozen and pumped out to remove hydrogen. The bottle was then allowed to warm to a temperature that still trapped any water but allowed sufficient pressure to fill the main mix tank with HF. Matheson research grade argon was then

introduced into the mix tank via the closed tube made with pinholes which was used to ensure adequate mixing of the gases. Mixes were normally prepared at total pressures of about 800 torr at 2% to 5% HF.

Prior to preparation of the gas mixture, the gas-handling system was evacuated and the pressure monitored by a thermocouple gauge. System pressure was normally about 0.1 torr which was the limit of the mechanical pump. The Heraeus gauge was used to monitor the pressure while filling the mix tank with HF and the Heise gauge was used to monitor the pressure of the argon as the mix tank was filled to its final pressure.

APPENDIX B

THE HF PIN LASER

The HF pin laser used in this experiment was critical in the initial development of the correct techniques for handling hydrogen fluoride gas. After the correct procedures were developed, the laser was used to perform two functions. First, after a new gas mixture was prepared, the laser was used to monitor the passivation of the test cell and its associated plumbing. Second, the laser was used as the primary method of determining the partial pressure of HF in the cell during a run when the gas was being pumped by the YALO laser.

The HF laser, commonly called a pin laser because of the construction of the electrode assembly, is shown in Figure B.1. It is similar to that described by Marcus and Carbone (1971). It was constructed from a lucite tube 27 inches long with a one inch I. D. and 1/4 inch wall thickness. The ends of the tube were cut at the Brewster angle and the windows were made of Infrasil (IR grade quartz), sealed in place with RTV Silastic compound. A mixture of SF₆ and H₂ entered the tube near both ends and was pumped from a central port of means of a mechanical pump. The laser was relatively insensitive to total gas pressure, but it was

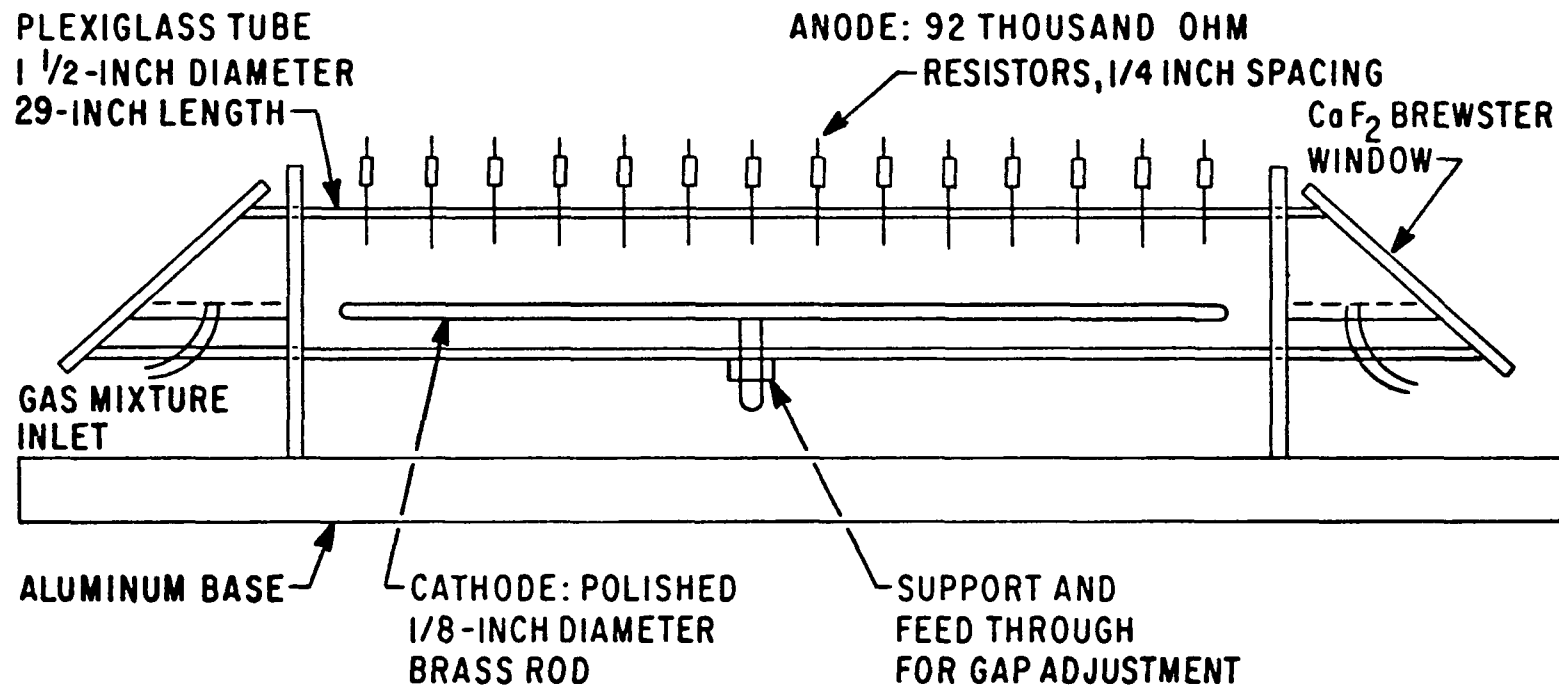


Figure B.1 The HF Pin Laser

determined that it operated most efficiently at a SF₆ to H₂ pressure ratio of ten. The gas flow was regulated by a separate throttling valve for each gas. Typical pressures in the tube were 25 torr of SF₆ and 2.5 torr of H₂.

The electrical circuitry that was used for operation of the laser is shown schematically in Figure B.2. The electrical discharge was generated by means of a 1000pf capacitor that was charged to approximately 14KV and discharged through the tube by means of a spark gap. The anode consisted of 92 one-kilohm resistors spaced 1/4 inch apart with their inner ends located 1/2 inch from a 1/8 inch diameter brass rod that formed the cathode. A pulse generator was used to activate the trigger circuit and firing frequency was normally set at two pulses per second.

There was no attempt made at a line selection within the cavity as is commonly accomplished by using an intracavity grating as the rear reflector. In this case the totally reflecting mirror was gold coated and had a 78 inch radius of curvature (the mirrors are not shown in Figure B.1). The output coupler was a calcium fluoride substrate coated for 30% reflection at 2.7 μ m. The distance between the mirrors in the cavity was 39 inches.

No actual energy measurements were made of the laser output. However, based on a typical operating efficiency of

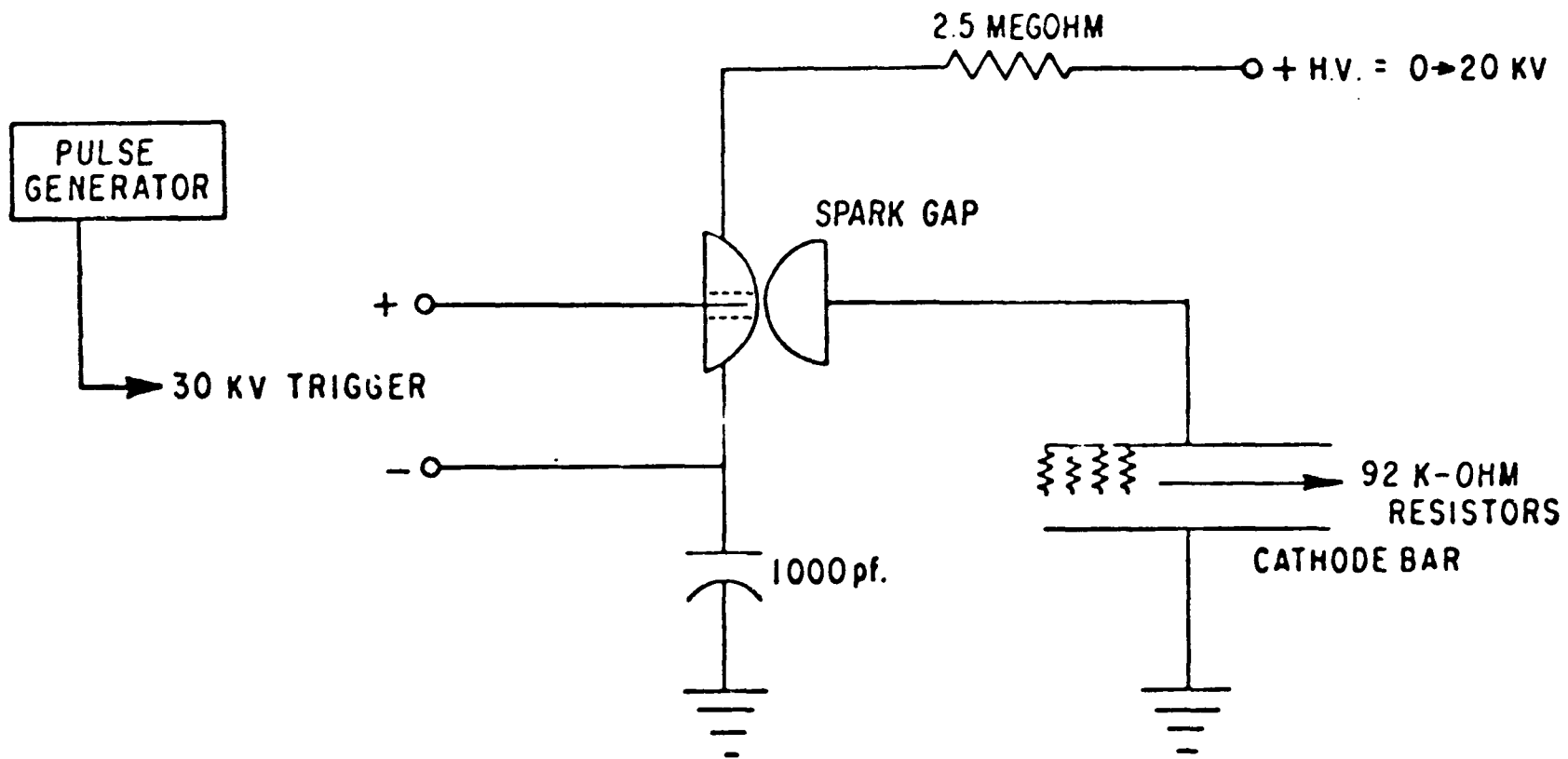


Figure B.2 The HF Pin Laser Circuit

0.1%, the average pulse contained approximately 0.1 millijoules of energy. Half-maximum pulse widths were normally on the order of a few μ sec. The total fluorescence signal generated by pin laser with one torr partial pressure in the HF cell was normally greater than 100mv. With an R-branch filter (2.0 μ m to 2.45 μ m) the signal was typically 30mv.

APPENDIX C

THE INFRARED DETECTION SYSTEM

The infrared fluorescence was monitored by a Texas Instruments indium-antimonide photovoltaic detector operating at liquid nitrogen temperature. Details of the detector assembly are shown in Figure C.1. The detector contained its own dewar for liquid nitrogen. The LN_2 was added by means of a Tygon tube sealed to the top of the detector with silicone rubber. This technique for filling the dewar, in addition to being convenient, protected the fragile pin terminals of the detector from the LN_2 . Precautions also had to be taken to ensure that any moisture accumulation was removed from the dewar prior to the initial filling with LN_2 as this could also lead to damage.

Primary light gathering in the system was accomplished by means of a two-inch diameter, five-inch focal length, calcium fluoride lens which was mounted directly above the upper cell window. The fluorescence image gathered by the main lens was focused down to the size of the detector chip by means of a one-inch diameter, one-inch focal length CaF_2 lens. The optical system was optimized by maximizing the signal output of the detector while the lenses were

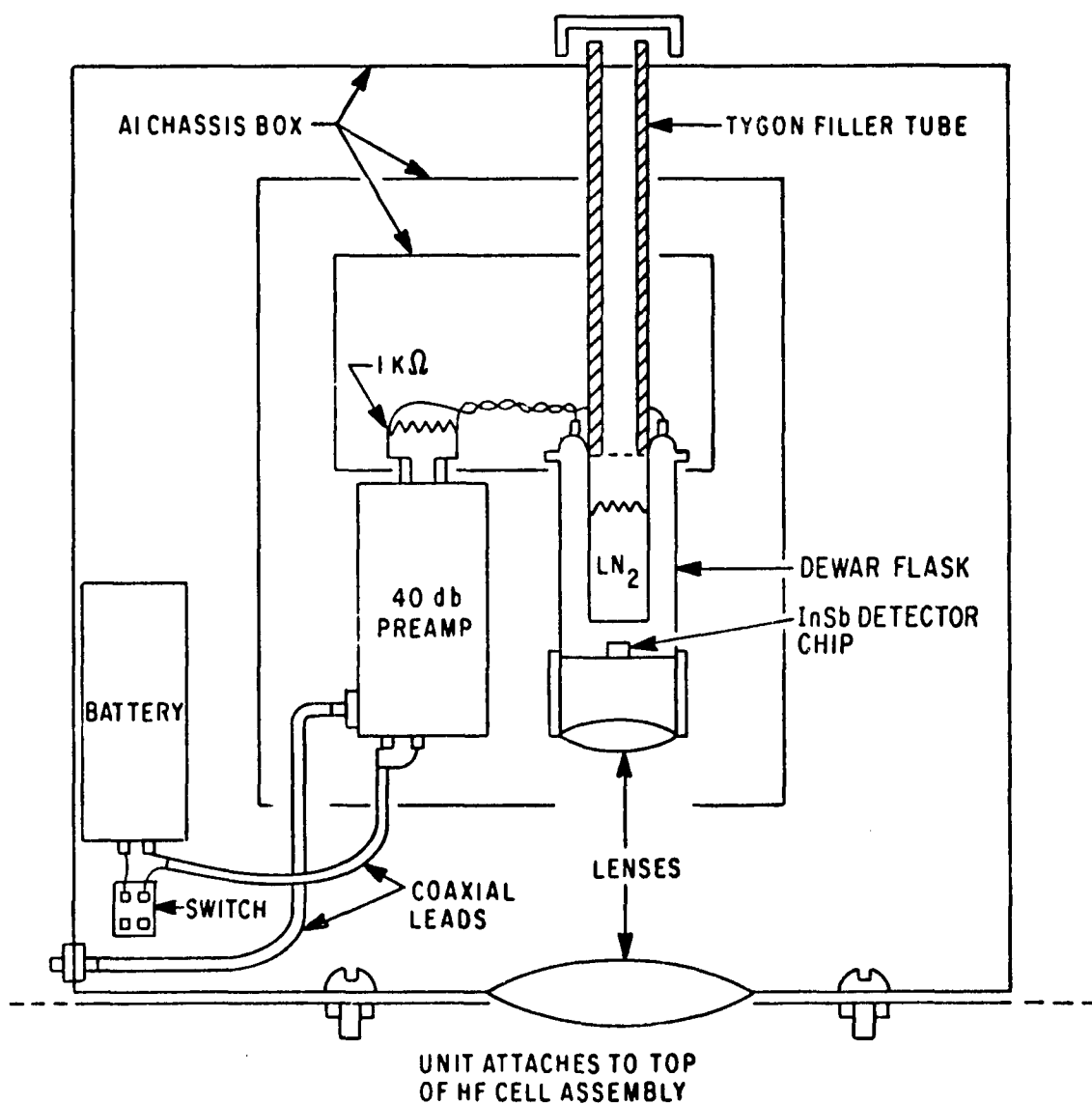


Figure C.1 The IR Detector Assembly

tried in varying positions. The HF pin laser provided the fluorescence for this procedure.

Some problems were experienced in reducing the intensity of scattered $1.35\mu\text{m}$ laser radiation reaching the detector. All interior surfaces of the assembly were blackened to reduce scattered laser light. Also care was taken to tightly enclose the detector to alleviate the scattered light interference.

Electrical noise generated by the firing of the laser in the immediate vicinity of the detector presented a problem in a sensitive electronic system of this nature. The arrangement used in this experiment proved to be very satisfactory. Noise signals from external sources were not usually observed and the limiting detection level of the system was limited by the 2 mv noise level of the detector preamplifier. The three aluminum chassis boxes were constructed such that the innermost box, to which the detector base was fastened, was electrically connected to the outer box and a common ground. The middle box was electrically insulated from the other two.

A 1000-ohm load resistor was used on the output terminals of the detector and the signal across this resistor was amplified by a Perry Associated Model 50 amplifier. This ultra-low-noise amplifier has a 40 DB gain and is biased with a 12 volt power supply. In this case power was supplied

by two six-volt batteries mounted within the detector assembly. By observing the decay rate of a non-pumping laser pulse, the time constant of the overall detector system was determined to be less than one μsec .

APPENDIX D

CALCULATION OF THE ENERGY REQUIREMENTS OF THE EXCITATION LASER

This appendix contains all of the essential elements of a calculation made to determine the energy requirements of the excitation laser. The first step is to calculate the amount of laser energy that is absorbed by HF gas. Next, the optics of the HF cell window and the infrared detector assembly are considered. Finally, the amount of radiation striking the detector is converted into an output voltage.

For the low HF gas pressures used in this work, the HF absorption line is predominately doppler broadened. According to the classic radiation text, Mitchell and Zemanski (1934), the peak absorption coefficient, $k_0(\text{cm}^{-1})$, is

$$k_0 = \frac{2}{\Delta\nu_D} \sqrt{\frac{\ln 2}{\pi}} \frac{\lambda_0^2}{\pi} \frac{g_1}{g_2} A_{2,0} N_T \quad (\text{D.1})$$

where λ_0 = the wavelength of the laser radiation in cm,
 g = a statistical weight factor which here is such that $g_2/g_1 \approx 1$, $A_{2,0}$ = the Einstein coefficient which represents the probability per second that the molecule will undergo a spontaneous transition between levels $V=2$ and $V=0$,

N_T = the total number of molecules per cm^3 , and $\Delta\nu_D$ = the Doppler width of the line in hertz. It will be necessary to calculate $\Delta\nu_D$ first. It can be calculated from the equation [again from Mitchell and Zemanski (1934)]

$$\Delta\nu_D = \frac{2\sqrt{R_0 \ln 2}}{\lambda_0} \frac{T}{W} \quad (\text{D.2})$$

where R_0 = the universal gas constant, 8.31×10^7 ergs/ $^\circ\text{K}$, T = the absolute temperature in $^\circ\text{K}$, and W = the molecular weight of the gas in grams/mole. Using the value of $\lambda_0 = 1.34 \mu\text{m}$ for the $\Delta V=2$ transition this gives

$$\Delta\nu_D = 600 \text{ MHz} = 6 \times 10^8 \text{ sec}^{-1}$$

According to a calculation by Meredith and Smith (1971), for $\text{HF}(V=0 \rightarrow 2)$, $A_{2,0} = 13 \text{ sec}^{-1}$. Substituting values into Equation D.1 gives

$$k_0 = 1.5 \times 10^{-17} N_T$$

Since absorption occurs only on one rotational level of the ground vibrational level, the number of absorbers must be calculated for $T=300^\circ\text{K}$. In this case the excitation laser can only excite the $V=0, J=6$ level (see Figure 2.3). From tabulated values such as those plotted in Figure 2.4, the population of this level is

$$N(V=0, J=6) = 0.02N_T.$$

That is, 2% of the HF molecules are available for excitation. Then Equation D.4 becomes

$$k_o(V=0, J=6) = 3 \times 10^{-19} N_T \text{cm}^{-1}.$$

At 300°K the value of N_T is given by

$$N_T = 3.2 \times 10^{16} \text{ cm}^{-3} \text{ torr}^{-1}.$$

Taking the partial pressure of HF in the cell to be 1 torr, the absorption coefficient becomes

$$k_o = 9.6 \times 10^{-3} \approx 10^{-2}.$$

Since the area of the InSb detector chip is approximately 1mm^2 , a corresponding size HF gas volume of 1mm^3 will be used. Then the fraction of the energy of the laser beam absorbed in this $X=1\text{mm}$ path length is

$$\begin{aligned} \text{Energy Fraction Absorbed} &= 1 - e^{-k_o X} = 1 - e^{-10^{-3}} \quad (\text{D.3}) \\ &= 0.0010. \end{aligned}$$

For convenience in the calculation, the energy of the excitation pulse reaching the gas sample is taken to be 1 millijoule, then 1 microjoule is absorbed by the sample.

This assumes that all of the excitation pulse energy is contained within the linewidth of the HF. However, the HF(V=0→2) linewidth is narrow compared with the spectral width of the laser pulse. For the HF gas, $\Delta\nu_D = 600 \text{ MHz} = 0.04\text{\AA}$, and the laser pulse was on the order of 0.5\AA as a minimum value. Hence, the energy absorbed from the one millijoule pulse becomes approximately 10^{-7} joules.

To find the number of radiating molecules, assume that each absorbed photon yields an HF(V=2) molecule. Then the energy per photon is

$$E_p = hc/\lambda_o = 1.5 \times 10^{19} \text{ joule}, \quad (\text{D.4})$$

where h = Planck's constant = 6.62×10^{-27} erg-sec, and c is the velocity of light. Hence, the number of excited molecules is

$$N_E = \frac{10^{-7}}{1.5 \times 10^{-19}} = 6 \times 10^{11} \text{ molecules}$$

The peak radiation rate from the 1mm^3 sample, R_p , is given by the relation

$$R_p = A_{2,1} N_E \text{ photons per sec.} \quad (\text{D.5})$$

Again using Meredith and Smith's calculations the value of

$A_{2,1}$ for HF(V=2→1) is 200 sec^{-1} . Substituting the values gives

$$R_p = 1.2 \times 10^{14} \text{ photons per sec.}$$

Using $\lambda_{2,1} = 2.7 \mu\text{m}$ for the wavelength of this transition, the peak power is

$$P_o = R_p hc / \lambda_{2,1} = 8.4 \times 10^{-6} \text{ watts.} \quad (\text{D.6})$$

This power is radiated into 4π steradians, and the amount reaching the detector depends upon the cell optics. The limiting aperture is the cell window. The fraction of the power reaching the detector is the area of the window divided by $4\pi d^2$ where d is the cell half thickness, i.e. the distance from the radiating volume to the window. In this case, the fraction of the power reaching the detector is 0.03 and from above, the peak power on the detector is

$$P_D = 2.5 \times 10^{-7} \text{ watts.}$$

The responsivity of the InSb detector is typically $R_s = 10^4$ volts/watt. Thus, the peak voltage signal from the detector is

$$V_0 = 1 \text{ millivolt.}$$

This is the expected output of the detector for a one-millijoule laser pulse. The normal output energy of the laser was approximately 70 millijoules. However, this output voltage is based on optimum conditions and no losses, such as reflection losses at the window for example. Also, a $2.7\mu\text{m}$ band-pass filter is used to attenuate the $1.34\mu\text{m}$ radiation of the excitation laser and it attenuates the fluorescence by approximately 30%. The most significant factor, however, is the temporal energy dilution of the laser pulses since in a typical long pulse mode the energy output takes place over a time of from 50 to $100\mu\text{sec}$.

LIST OF SYMBOLS

°	
Å	angstrom unit (10^{-10} m)
$A_{2,0}$	Einstein coefficient, (V=2→0) transition
$A_{2,1}$	Einstein coefficient, (V=2→1) transition
C	a constant, eq. 2.6
c	velocity of light
D	any diatomic molecule
DB	decibel
d	HF cell half thickness
E_p	energy per photon
e	exponential
exp	exponential
F	fluorine
g	statistical weight factor
HF	hydrogen fluoride
h	Planck's constant
I	fluorescence intensity
I_0	initial fluorescence intensity
J	rotational quantum number
K_v	rate constant
K	a constant, eq. 2.6
°K	absolute temperature, degrees kelvin
KV	kilovolt
k	any positive integer

k_0	absorption coefficient
LN_2	liquid nitrogen
M	any molecule
mv	millivolt
N	number of molecules per cm^3
$Nd:YALO$	neodymium doped yttrium orthoaluminate crystal
N_T	total number of molecules per cm^3
N_E	number of vibrationally excited molecules
n	any positive integer
P	pressure
P_0	peak power radiated
$P(J)$	a vibrational-rotational transition where $\Delta J=+1$ in emission
P_D	peak power reaching the detector
R	rotation
R_0	universal gas constant
R_S	InSb detector responsivity
$R(J)$	a vibrational-rotational transition where $\Delta J=-1$ in emission
R_p	peak radiation rate
T	translation in (V-T) and (V-R-T) only
T	absolute temperature, °K in all equations
t	time
V	vibrational quantum number
V_0	detector output signal

W	molecular weight
X	distance along laser beam
γ	rate constant
ΔJ	change in the rotational quantum number
ΔV	change in the vibrational quantum number
$\Delta \nu_0$	linewidth of a spectral line
$\Delta \nu_D$	doppler broadened linewidth
λ	wavelength
λ_0	wavelength of laser at $1.34\mu\text{m}$
μm	micrometer (10^{-6}m)
τ	relaxation time

REFERENCES

- Airey, J. R. and S. F. Fried, "Vibrational Relaxation of Hydrogen Fluoride," *Chemical Physics Letters*, Vol. 8, number 1, 1971, pp. 23-26.
- Bloom, A. L., "Observation of New Visible Gas Laser Transitions by Removal of Dominance," *Applied Physics Letters*, Vol. 2, number 5, 1963, pp. 101-102.
- Bott, J. F., "HF Vibrational Relaxation Measurements by the Combined Shock Tube - Laser Induced Theoretical Technique", Aerospace Report No. TR-0172(2754)-2, El Segundo, California, 1972.
- Bott, J. F. and N. Cohen, "Shock Tube Studies of HF Vibrational Relaxation", *The Journal of Chemical Physics*, Vol. 55, 3698, 1971.
- Chen, H. and C. B. Moore, "Vibration→Rotation Energy Transfer in Hydrogen Chloride", *The Journal of Chemical Physics*, Vol. 54, number 9, 1971. pp. 4072-4080.
- Chester, A. N., "Chemical Lasers: A Status Report," *Laser Focus*, Nov. 1971, p. 25.
- Farmer, G. I., B. G. Hugh, L. M. Taylor and M. R. Kagen, "Concentration and Dye Length Dependence of Organic Cye Laser Spectra," *Applied Optics*, Vol. 8, 1969, pp. 363-367.
- Fried, S. S., J. Wilson and R. L. Taylor, "Measurement of the Temperature Dependence of the Vibrational Relaxation Rate of HF and the Effect of SF₆, N₂, F₂, as Diluents," unpublished report, Avco Everett Research Laboratory, Everett, Massachusetts (n.d.).
- Herget, W. F., W. E. Deeds, N. M. Gailer, R. J. Lovell and A. H. Nielsen, "Infrared Spectrum of Hydrogen Fluoride: Line Positions and Line Shapes. Part II Treatment of Data and Results," *Journal of the Optical Society of America*, Vol. 52, number 10, 1962, pp. 1113-1119.
- Hocker, L. O., M. A. Kovacs, C. K. Rhodes, G. W. Flynn, and A. Javon, "Vibrational Relaxation Measurements in CO₂ Using an Induced-Fluorescence Technique,

Physics Review Letters, Vol. 17, number 5, 1966,
pp. 233-235.

- Jonathan, N., C. M. Mellior-Smith and D.H. Slater, "Initial Vibrational Energy Level Populations Resulting from the Reaction $H+F_2$ as Studied by Infrared Chemiluminescence," *The Journal of Chemical Physics*, Vol. 53, number 11, 1970, pp. 4396-4397.
- Kushida, T., "Linewidths and Thermal Shifts of Spectral Lines in Neodymium-Doped Yttrium Aluminum Garnet and Calcium Fluorophosphate," *Physical Review*, Vol. 185, number 2, 1969, pp. 500-508.
- Landau, L. and E. Teller, "Zur Theorie der Schalldispersion." *Physik z. Sowjetunion*. g.10, h.1, 1936, p. 34.
- Mann, D. E., B. A. Thrush, D. R. Lide, Jr., J. J. Ball and N. Acquista, "Spectroscopy of Fluorine Flames. I. Hydrogen-Fluorine Flame and the Vibration-Rotation Emission Spectrum of HF.," *The Journal of Chemical Physics*, Vol. 34, number 2, 1961, pp. 420-431.
- Marcus, S. and R. J. Carbone, "Performance of a Transversely Excited Pulsed HF Laser," project report No. LTP-11, MIT Lincoln Lab, 1971.
- Meredith, R. E. and F. G. Smith, "Investigations of Fundamental Laser Processes," University of Michigan, Willow Run Laboratories, Report No. 84130-39-T(11), 1971.
- Mitchell, A. C. and M. W. Zemanski, "Resonance Radiation and Excited Atoms," Cambridge University Press, 1934.
- Moore, C. B., R. E. Wood, B. L. Hu and J. T. Yardley, "Vibrational Energy Transfer in CO_2 Lasers," *The Journal of Chemical Physics*, Vol. 46, number 11, 1967, pp. 4222-4231.
- Morozov, A. M., M. N. Tolstoi, P. P. Feofilov and V. N. Shapovalov, "Luminescence and Stimulated Radiation of Neodymium in Lanthanum-Sodium Molybdate Crystals," UDC 535.372: 548.0, 1966, pp. 224-226.
- Pearson, A. D., S. P. S. Porto and W. R. Northover, "Laser Oscillations at 0.918, 1.057, and 1.401 Microns in Nd^{3+} -Doped Borate Glasses," *Journal of Applied Physics*, Vol. 35, number 6, 1964, pp. 1704-1706.

- Polanyi, W. J., K. G. Anlouf, P. E. Charters, D. S. Horne, R. G. Macdonald, D. H. Maylotte, W. J. Skrlac, D. C. Tardy and K. B. Woodall, "Translational Energy-Distribution in the Products of Some Exothermic Reactions," *The Journal of Chemical Physics*, Vol. 53, number 10, 1970, pp. 4091-4092.
- Shin, H. K. "Vibrational-Rotation-Translation Energy Transfer in HF-HF and DF-DF," *Chemical Physics Letters*, Vol. 10, number 1, 1971, pp. 81-85.
- Smith, R. G., "New Room Temperature CW Laser Oscillations In Nd:YAG," *IEEE Journal of Quantum Electronics*, 1968, p. 506.
- Snitzer, E., "Glass Lasers," *Applied Optics*, Vol. 5, 1966, pp. 1487-1499.
- Solomon, W. C., J. A. Blauer, F. C. Jaye and J. G. Hnat, "The Vibrational Excitation of HF Behind Incident Shock Waves," *International Journal of Chemical Kinetics*, Vol. 3, 1971, p. 215.
- Weber, M. J. and T. E. Varitimos, "Optical Spectra and Intensities of Nd³⁺ in YA10₃," *Journal of Applied Physics*, Vol. 42, number 12, 1971, pp. 4996-5005.